Ecole de Mines de Saint Etienne
158, Cours Fauriel
42100 Saint Etienne
FRANCE

Technische Universität Berlin
Straße des 17. Juni 135
10623 Berlin
GERMANY

as a visiting student
at the Solar Energy Laboratory
of the University of Wisconsin - Madison

Experimental Validation of Photovoltaic Pumping System Models

Experimentelle Untersuchung von Modellen photovoltaischer Pumpsysteme

Vérification Expérimentale de Modèles de Systèmes de Pompage d'Eau Photovoltaïque

by Dagmar Jähnig

Travail de Fin d'Etudes
Diplomarbeit

Madison, 1997

Abstract

An experimental setup has been designed that allows measuring the performance of small direct coupled photovoltaic water pumping systems. Minute by minute data of flow rate, radiation, ambient and cell temperatures as well as voltage and current have been recorded for several days of outdoor operation. A DC circulating pump and two PV panels from different manufacturers have been used. The measurements were made at a constant static head and using either one of the two PV panels.

Predictions of the performance of the system use a 4 parameter PV model described by Duffie and Beckman [4] and a model by Kou [8] that describes pump and motor with two equations curve fitted from manufacturer's data. Both models use only manufacturer's data to predict the performance of the system. For the predictions measured radiation and temperature data have been used. The results of predictions and experiments have been compared.

Significant differences have been found between predictions and measurements. The influence of the two models and of bad parameters for the models is discussed in this thesis.

The influence of incorrect model parameters in the pump/motor model has been found to be greater in the PV model. The quality of the manufacturer's data varies significantly. Some manufacturers test each outgoing panel and the measured parameters can vary substantially from the catalog data. Radiation measurements made with a pyranometer do not necessarily represent the radiation actually absorbed by the PV cells because of incidence angle effects on the reflection off the cover of the cells. These effects depend very much on the material used as a cover.

Zusammenfassung

Eine Versuchsapparatur, mit der photovoltaische Pumpsysteme getestet werden können, wurde entworfen. Bei den Anlagen, die in dieser Arbeit betrachtet werden, handelt es sich um ein PV Modul, das direkt an eine Pumpe, die mit Gleichstrom betrieben wird, angeschlossen wird. Die Anlage besitzt keinen Batteriespeicher. Für die Versuche wurde Wasser aus einem Behälter duch ein Druchflußmeßgerät wieder in den Behälter gepumpt.

Mehrtägige Versuche in Freien wurden durchgeführt, wobei Volumenstrom, Strom, Spannung, Solarstrahlung und Umgebungs- und Zelltemperatur in Abständen von einer Minute gemessen wurden. Es wurden eine Gleichstromkreiselpumpe und zwei Solarmodule verschiedener Hersteller verwendet. Messungen wurden bei konstanter statischer Pumphöhe mit jeweils einem der beiden Solarmodule gemacht.

Zur Berechnung des zu erwartenden Volumenstroms wurden ein 4-Parameter Modell für die Solarzellen verwendet sowie ein Modell, das das Verhältnis von Volumenstrom, Strom, Spannung und Pumphöhe mit zwei Gleichungen beschreibt, deren Parameter den Herstellerangaben angepaßt werden müssen. Für beide Modelle genügen Herstellerangaben, keine Tests sind nötig, um Parameter zu bestimmen. Der zu erwartende Volumenstrom wurde für den jeweiligen Testtag berechnet, wobei Meßwerte für Solarstrahlung und Zelltemperatur verwendet wurden. Die Ergebnisse wurden dann mit den Meßergebnissen verglichen.

Deutliche Differenzen zwischen den berechneten und gemessenen Werten wurden festgestellt. Der Einfluß der beiden Modelle beziehungsweise der Modellparameter wird in dieser Arbeit diskutiert.

Es wurde festgestellt, daß inkorrekte Modellparameter für das Pumpenmodell einen größeren Einfluß als inkorrekte Parameter für das Solarzellenmodell haben. Die Qualität der Herstellerangaben ist sehr unterschiedlich. Einige Hersteller testen jedes hergestellte Solarmodul. Die dabei gemessenen Parameter können sich erheblich von den Katalogangaben unterscheiden.

Ergebnisse von Solarstrahlungsmessungen entsprechen nicht immer der tatsächlich von den Solarzellen absorbierten Strahlung. Der Anteil der Solarstrahlung, der von der Abdeckung der Solarzellen reflektiert wird, kann erheblich vom Winkel abhängen, mit den das Licht auf die Solarzellen fällt. Dieser Effekt hängt allerdings sehr von Material der Abdeckung ab und konnte in dieser Arbeit nur abgeschätzt werden.

Acknowledgments

First of all I would like to thank everybody who made it possible for me to come to Madison to do a research project in the Solar Energy Lab. *Prof. Kraume* and *Patrick Mier* from the Technical University of Berlin, didn't mind that I turned a French-German exchange program into a three country program. *Michel Cournil*, my advisor in France, encouraged me to do this unusual step and go to a third country to finish my studies. *Prof. Bill Beckman*, the director of the Solar Energy Lab, invited me to come to the Solar Energy Lab and treated me as if I was a regular graduate student in the lab.

I also would like to thank the *Ecole de Mines de St-Etienne* and the *Fondation FI3M* who helped to finance the trip to and my stay in Madison.

Thanks to my three advisors in the Solar Energy Lab, Prof. Bill Beckman, Prof. John Mitchell and Prof. Sandy Klein, a special thanks to Sandy for all your help with EES (you were always ready to help, even making a new version of EES so I could do unusual tasks like copying big tables with minute data for a whole day!) and for reading the drafts of this thesis.

I also would like to thank all students in the Solar Lab for a great working atmosphere and a great time in Madison, especially Svein for the always helpful conversations about PV Cells.

Table of Contents

List of Figures

List of Tables

Nomenclature

Sign	Description
A, a	Curve fitting parameter (PV model), Area
a_0	Curve fitting parameter for the pump/motor model
a_1	Curve fitting parameter for the pump/motor model
a_2	Curve fitting parameter for the pump/motor model
a_3	Curve fitting parameter for the pump/motor model
b	Curve fitting parameter
b_0	Curve fitting parameter for the pump/motor model
b_1	Curve fitting parameter for the pump/motor model
b_2	Curve fitting parameter for the pump/motor model
b_3	Curve fitting parameter for the pump/motor model
b_4	Curve fitting parameter for the pump/motor model
b_5	Curve fitting parameter for the pump/motor model
b_6	Curve fitting parameter for the pump/motor model
b_7	Curve fitting parameter for the pump/motor model
b_8	Curve fitting parameter for the pump/motor model
b_9	Curve fitting parameter for the pump/motor model
b_{10}	Curve fitting parameter for the pump/motor model
d	Diameter
E_q	Bandgap of cell material
G	Gravitational constant
G	Solar Radiation
H	Head loss

H	Pump head
I	Current
I_D	Diode current
I_L	Light current
I_m	Current at the maximum power point
I_0	Diode reverse saturation current
I_{sc}	Short circuit current
L	Length
M	Flow rate
N	day of the year
N_s	Number of cells in series in one module
p	Number of cells in parallel in an module
P	Power, number of modules in parallel in an array
R	Resistance
Re	Reynolds Number
R_s	Series resistance
R_{sh}	Shunt resistance
rms	Root mean squares
s	Number of cells in series in a module
S	Number of modules in series in an array
SSQ	Sum of squares
T	Temperature
T_a	Ambient Temperature
T_c	Cell temperature

U_L	Overall heat loss coefficient
v	velocity
V	Voltage
V_m	Voltage at the maximum power point
V_{oc}	Open circuit voltage

Greek Symbols

α	Absorptance of the cells
δ	Declination angle
η_c	Cell efficiency
θ	Incidence angle
μ_{voc}	Temperature coefficient of voltage
μ_{Isc}	Temperature coefficient of current
ν	Viscosity
ρ	Density
τ	Transmittance of the cover of the cells
ϕ	Latitude
ω	Hour angle

Subscripts

ex	existing
m	at the maximum power point
n	new
oc	Open circuit
ref	at reference conditions
sc	Short circuit

A Introduction

A.1 Background

Conventional energy use like burning fossil fuels is based on using up resources that have been built up on earth over millions of years. This is a non-sustainable process because those resources are renewed much more slowly than they are consumed. Also burning fossil fuels causes air pollution and releases gases that contribute to the greenhouse effect. Nuclear energy does not pollute directly but there is a danger of possible accidents and the problem of safe waste storage.

Sooner or later we will have to find a way to satisfy our energy needs in a sustainable way. Solar energy is one technology that could play an important role.

Every day the earth receives far more free energy from the sun than we consume. We only have to be able to convert it into energy forms that we can use and that can be stored for use at night or in winter. This energy conversion also has to be affordable. Solar energy is generally more expensive than energy obtained from conventional sources. However, these energy prices do not account for the effects on the environment or on human health.

One form of solar energy conversion is photovoltaic cells. They convert solar radiation directly into electricity that can be stored in batteries or used in direct-coupled systems. The technology is very reliable because there are no moving parts. PV arrays can work in remote locations without technical assistance for a long time.

Commercially available PV cells are still very expensive because of their low efficiency of about 10-12%. Another problem is the high energy consumption during the manufacturing process. There are also storage problems with batteries for stand alone systems.

A very promising application of solar energy in general and PV cells in particular is direct-coupled PV pumping systems because in this application, the storage problem is eliminated by storing pumped water in tanks instead of electrical energy in batteries. For

irrigation purposes the availability of solar energy and the need of water pumping coincide very well.

Another application for direct-coupled PV pumping systems is a solar domestic hot water system. Pumping power is needed when the water in the solar collector is hot. A PV driven pump would work only when there is enough solar radiation to heat the collector. The PV panel would therefore work as energy source and controller at the same time. It also controls the flow rate depending on the radiation level. Storage is not needed in this system.

A.2 Motivation for Research

Models for PV cells and for pump and motor have been developed so that the performance of the whole system can be predicted using only manufacturer's information. But are those predictions good enough? Can we actually size a system that matches our energy needs only with manufacturer's information? For an application like a solar domestic hot water system where the PV panel also acts as a controller and the flow rate pumped at a certain radiation level should make the thermal collector work efficiently, prediction have to be fairly accurate.

Measurements will therefore be made using a small direct-coupled PV pumping scheme that could be used in a solar domestic hot water system. Predictions can then be compared with the measurements. Measured data for radiation and temperature will be used to predict the performance of the system.

B PV Cells

B.1 Introduction

Photovoltaic cells are semiconductor devices that convert solar radiation directly into electricity. The most common cells are made out of two layers of silicon. On one side of the junction, the silicon is doped with a small amount of boron (p-silicon) and on the other side with a small amount of phosphorus (n-silicon). Phosphorus has an extra electron in its outer shell while boron has one electron less than silicon. This creates a field across the junction.

When solar radiation is absorbed on the solar cell, electrons are freed from the outer shells (an electron-hole-pairs are created) and can move around. If an external circuit is attached to the cell, electrons and holes don't recombine spontaneously, current flows through that circuit because of the potential across the junction.

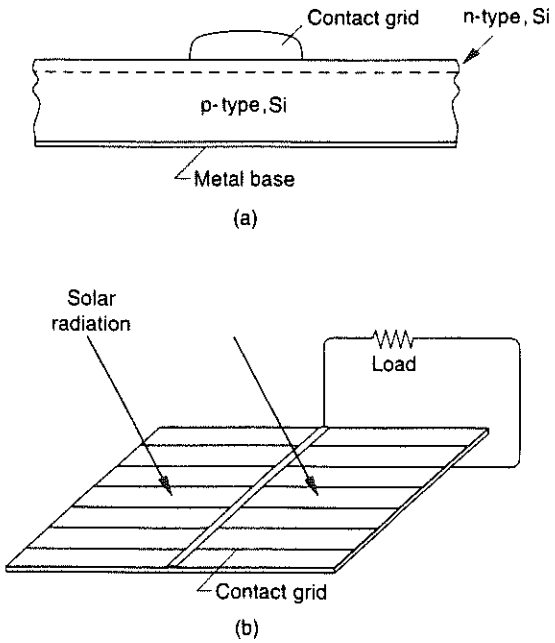

Figure B-1: (a) Section of a silicon solar cell. (b) Schematic of a cell, showing top contacts [4]

To form the external circuit the cells are attached to a metal base at the bottom and to a metal grid at the top that allows the solar radiation to penetrate to the silicon layer. A

cross-section of a PV cell and a cell connected to an external circuit are shown in Figure B-1.

B.2 PV Cell Model

To be able to predict the performance of the pumping system, a model for the PV module is to be found that allows calculating the current-voltage relationship of the module for varying radiation levels and ambient temperatures. Performance predictions should be possible without testing of the module using only data commonly known or given by the module manufacturer.

B.2.1 PV Cell Model at Reference Conditions

PV cells are non-linear power sources. Their current-voltage characteristic depends on the radiation level and the cell temperature.

A number of different equivalent circuits have been proposed to describe the current voltage relationship of photovoltaic cells. Rauschenbach [9], Townsend [11] and Eckstein [5] studied several different configurations. The most commonly used circuit seems to be the one shown in Figure B-2 which requires five cell parameters: the light current I_L, the diode reverse saturation current I_0, the series resistance R_s, the shunt resistance R_{sh} and a curve fitting parameter a. The model can describe the current-voltage relationship of a single cell or many cells connected in parallel or in series in modules or arrays. It is valid at a fixed solar radiation and cell temperature and is given by

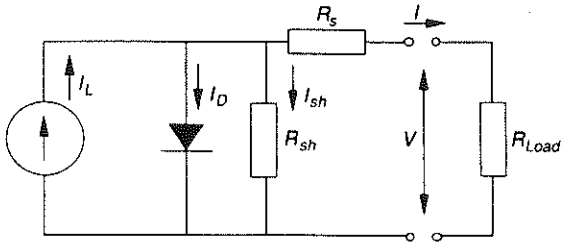

Figure B-2: Equivalent circuit for a PV generator [4]

$$I = I_L - I_D = I_L - I_0\left\{\exp\left[\left(V + IR_s\right)/a\right] - 1\right\} - \frac{V + IR_s}{R_{sh}} \qquad \text{(B-1)}$$

where

I - current of the cell, module or array

V - voltage of the cell, module or array

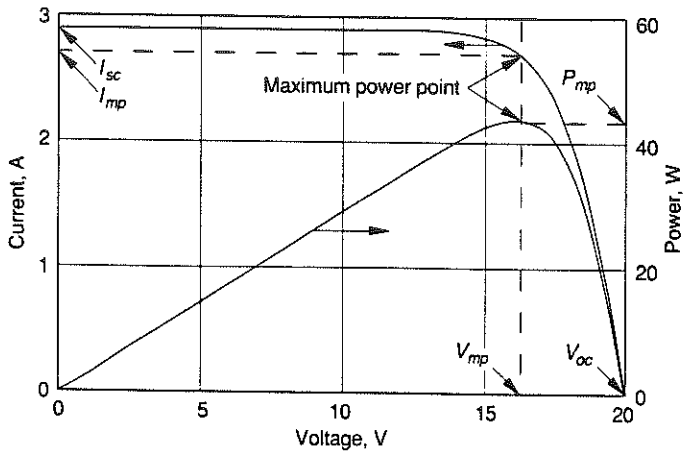

Figure B-3: Typical I-V Curve for a PV module [4]

A typical I-V curve is shown in Figure B-3. The power output P of the cell is given by

$$P=I*V \qquad \text{(B-2)}$$

The shunt resistance of most crystalline cells is very large so that the last term in equation (B-1) can be neglected for silicon cells. Only when the I-V curve has a significant slope at low voltages, the shunt resistance needs to be considered. This is the case for amorphous cells.

After this simplification the model becomes

$$I = I_L - I_0\left\{\exp\left[\left(V + IR_s\right)/a\right] - 1\right\} \qquad \text{(B-3)}$$

It now contains only four parameters. To determine those parameters the I-V values must be known at a minimum of four conditions. Those conditions could be any four current voltage pairs on the curve. See chapter G.1.1.4 for a curve fitting method using measured IV data. The manufacturers of solar cells usually make measurements of only three current-voltage pairs:

1) Open circuit voltage: V_{oc} (I_{oc}=0)

2) Short circuit current: I_{sc} (V_{sc}=0)

3) Maximum power point: V_m, I_m

The forth condition comes from the knowledge of the variation of short circuit current and open circuit voltage with temperature. Generally, the short circuit current increases and the open circuit voltage decreases with increasing temperature.

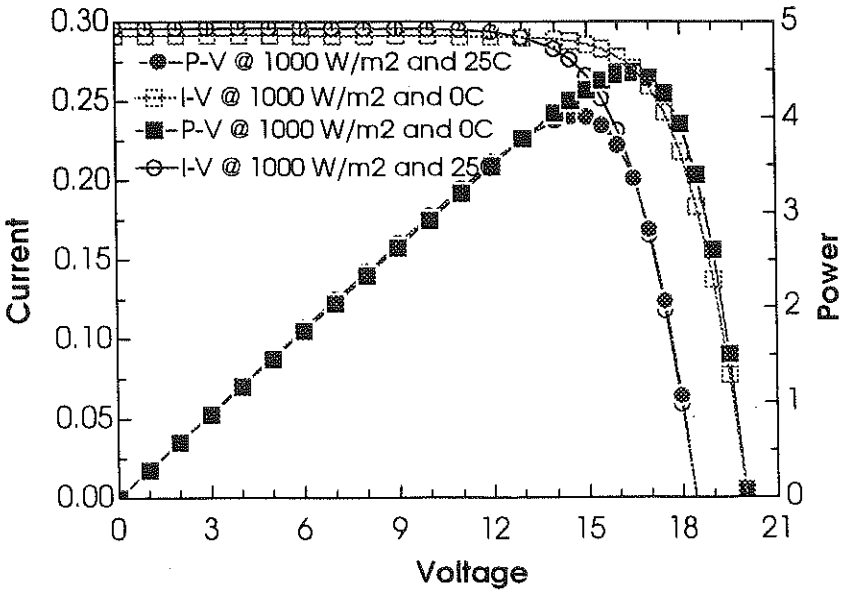

Figure B-4: I-V and P-V curves at different temperatures of the module SOLAREX MSX-5L using the manufacturer's parameters

$$\mu_{Voc} = \frac{dV_{oc}}{dT} = \frac{V_{oc}(T_2) - V_{oc}(T_1)}{T_2 - T_1} \qquad \text{(B-4)}$$

$$\mu_{Isc} = \frac{dI_{sc}}{dT} = \frac{I_{sc}(T_2) - I_{sc}(T_1)}{T_2 - T_1} \qquad \text{(B-5)}$$

These values are usually provided by the manufacturer. Because the open circuit current decreases more then the short circuit current increases, the power generally decreases with increasing temperature. These variations with temperature are shown in Figure B-4.

The four conditions lead to four independent equations which makes it possible to calculate the four model parameters:

1) At short circuit conditions, the voltage equals zero, the second term in the model equation becomes very small, and can be neglected. This leads to the very simple solution that the short circuit current equals the light current:

$$I_{sc} = I_L \tag{B-6}$$

2) At open circuit conditions, the current equals zero, the 1 is small compared to the exponential term and can therefore be neglected, and equation (B-3) becomes

$$I_L = I_0 \cdot \exp(V_{oc} / a) \tag{B-7}$$

3) Substituting V_m and I_m in equation (B-3) equation (B-7) as an expression for I_0 and also neglecting the 1 in equation (B-3) at the maximum power point, we get

$$R_s = \frac{a \cdot \ln\left(1 - \frac{I_m}{I_L}\right) - V_m + V_{oc}}{I_m} \tag{B-8}$$

4) Knowing the temperature coefficient of current and voltage a fourth independent equation can be found by equating the measured coefficients with the analytically determined definitions.

$$a = \frac{\mu_{Voc} T_c - V_{oc} + E_q N_s}{\frac{\mu_{Isc} T_c}{I_L} - 3} \tag{B-9}$$

where

E_q - bandgap of module material

N_s - number of modules in series in one module

B.2.2 Changing of Weather Conditions

The manufacturer's data are usually measured at Standard Test Conditions of 1 kW/m^2 radiation and a cell temperature of 25°C. Using equations (B-6) to (B-9) the four

cell parameters of the module operating at this conditions can then be determined. To be able to calculate the output of the PV module at different weather conditions, the cell parameters of the model need to be recalculated for existing operating conditions. As shown by Townsend [], the following approximations give good results for many PV modules:

$$I_L = \left(\frac{G}{G_{ref}}\right)\left\{I_{Lref} + \mu_{Isc}\left(T_c - T_{cref}\right)\right\} \quad \text{(B-10)}$$

$$\frac{I_0}{I_{0ref}} = \left(\frac{T_c}{T_{cref}}\right)^3 \exp\left[\frac{N_s E_q}{a_{ref}}\left(1 - \frac{T_{cref}}{T_c}\right)\right] \quad \text{(B-11)}$$

$$\frac{a}{a_{ref}} = \frac{T_c}{T_{cref}} \quad \text{(B-12)}$$

$$R_s = R_{sref} \quad \text{(B-13)}$$

where

T_c - cell temperature

T_{cref} - cell temperature at reference conditions

In this model the light current I_L and therefore the short circuit current I_{sc} is proportional to the radiation level but it varies also with the cell temperature. The reverse saturation current I_0 and the curve fitting parameter A also depend on the cell temperature.

B.2.3 Cell Temperature

The incident solar energy on a PV cell is converted only partly into electrical energy. The rest is converted into heat and it must be dissipated into the surroundings. The steady-state energy balance of the cell is therefore: the absorbed power equals the electric power plus the dissipated power. To calculate the dissipated power an overall heat loss coefficient is needed.

$$\tau\alpha \cdot G = \eta_c \cdot G + U_L\left(T_c - T_a\right) \tag{B-14}$$

$$T_c = T_a + \frac{G \cdot \tau\alpha}{U_L}\left(1 - \frac{\eta_c}{\tau\alpha}\right) \tag{B-15}$$

where

T_a - ambient temperature

τ - transmittance of the cover over the cells

α - absorptance of the module

η_c - cell efficiency

U_L - module overall heat loss coefficient

The cell efficiency is given by $\eta_c = \frac{P}{G \cdot Area}$ (B-16)

where

A - module area

If $\tau\alpha$ is not known, a value of 0.9 can be used without making a big error as the term $\eta_c/\tau\alpha$ is small compared to unity ($\eta_c \approx 0.1$). The heat loss coefficient UL varies with ambient temperature, radiation and wind speed. Often a default value of 27.69 W/m^{2}K is used which corresponds to a radiation level of 800 W/m^2, an ambient temperature of 20°C, a cell temperature of 46°C and 1 m/s wind speed. See chapter G.1.1.2 for further discussion of this topic.

B.3 Series/Parallel Groupings of Modules

PV modules can be connected in series and/or in parallel to obtain arrays. The PV model can represent a cell, a module or an array depending on the model parameters used. To calculate the I-V-characteristic of an array when the characteristic of a module is known the following equations can be used. The array voltage is proportional to the

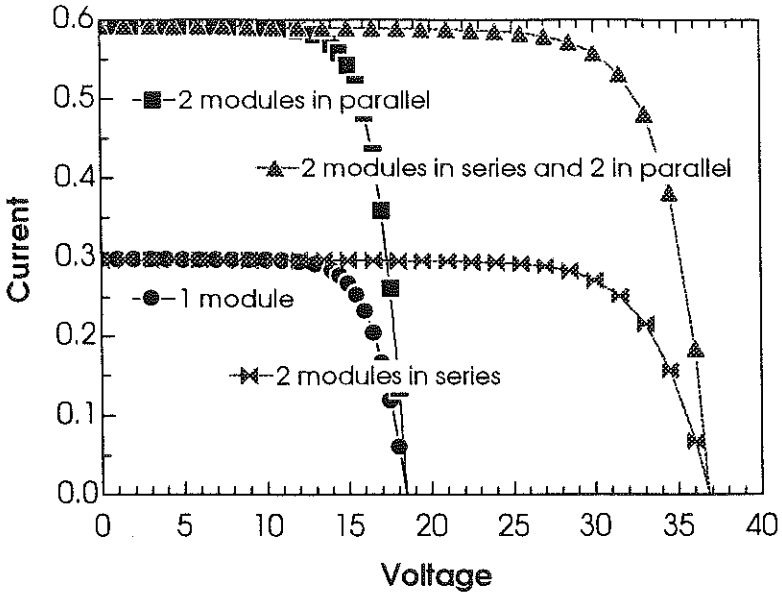

Figure B-5: Different series/parallel groupings of PV modules

number of modules connected in series, the array current is proportional to the number of modules connected in series. This is shown Figure B-5.

$$V_{array} = S \cdot V_{module} \quad \text{(B-17)}$$

$$I_{array} = P \cdot I_{module} \quad \text{(B-18)}$$

where

S -number of modules in series in the array

P - number of modules in parallel in the array

B.4 Rewiring an existing module

Given the I-V-model of an existing module, it is possible to calculate the characteristics of the separate cells. The characteristics of a different combination of these cells can then be determined. For this purpose, the model parameters for a single cell and afterwards for the new combination of cells need to be calculated.

The relationship of the open circuit voltages, short circuit currents and the maximum power points is the same as for groupings of modules in an array:

$$V_{module} = s \cdot V_{cell} \quad \text{(B-19)}$$

$$I_{module} = p \cdot I_{cell} \quad \text{(B-20)}$$

where

p - number of cells in parallel in one module

s - number of cells in series in one module

The temperature coefficients of voltage and current are sometimes given in amps and volts per degree Celsius respectively and sometimes in percent of open circuit voltage and short circuit current per degree Celsius. To determine the absolute values for a single cell, which are needed for the model, the percentage value must be applied to the new open circuit voltage and short circuit current. Table B-1 summarizes the calculations necessary for determining the model parameters when changing the parallel/series connections of a module.

Existing module	Single cell	"New" module
V_{oc}	V_{oc}/s_{ex}	$V_{oc} \cdot s_n/s_{ex}$
I_{sc}	I_{sc}/p_{ex}	$I_{sc} \cdot p_n/p_{ex}$
V_m	V_m/s_{ex}	$V_m \cdot s_n/s_{ex}$
I_m	I_m/p_{ex}	$I_m \cdot p_n/p_{ex}$
μ_{Isc} in %	$\mu_{Isc} * I_{sc}/p_{ex}$	$\mu_{Isc} \cdot I_{sc} \cdot p_n/p_{ex}$
μ_{Voc} in %	$\mu_{Voc} * V_{oc}/s_{ex}$	$\mu_{Voc} \cdot V_{oc} \cdot s_n/s_{ex}$
A	$A/s_{ex}/p_{ex}$	$A \cdot s_n \cdot p_n/s_{ex}/p_{ex}$

Table B-1: Calculations necessary for rewiring a module

B.5 Conclusion

Table B-2 shows the twelve parameters needed to calculate the I-V-characteristics of a module for a measured radiation and ambient or cell temperature.

	Parameters		Source
1	$V_{oc,ref}$	Open circuit voltage at reference conditions	manufacturer
2	$I_{sc,ref}$	Short circuit current at reference conditions	manufacturer
3	$V_{m,ref}$	Voltage at maximum power point at ref. conditions	manufacturer
4	$I_{m,ref}$	Current at maximum power point at ref. conditions	manufacturer
5	μ_{Voc}	Temperature coefficient of voltage	manufacturer
6	μ_{Isc}	Temperature coefficient of current	manufacturer
7	N_s	Number of cells in series in one module	manufacturer
8	G_{ref}	Radiation at reference conditions	manufacturer
9	T_{cref}	Cell Temperature at reference conditions	manufacturer
10	E_q	Bandgap of module material	default
11	$\tau\alpha$	Transmittance of cover, absorptance of module	default
12	U_L	Overall heat loss coefficient of module	default
	Measurements		
1	G	Radiation	
2	T_a or T_c		

Table B-2: Parameters and measurements necessary for the PV cell model

Given the first nine parameters by the manufacturer, the IV curve of a module can be calculated with the described model. The bandgap of the module material E_q is generally known as the bandgap of silicon. $\tau\alpha$ can be reasonably estimated. For discussion of the heat loss coefficient see chapter G.1.1.2.

The quality of the results with this model will depend significantly on the accuracy of the manufacturer's data. The influence of module parameters on the output of the model and on predictions of the flow rate of a direct coupled water pumping system will be discussed in the following chapters.

C Pump/Motor

C.1 Introduction

The DC current generated by the PV module is converted into mechanical energy by the motor which is then converted into hydraulic energy by the pump. A method to calculate the pump-motor system as one unit using manufacturer's data was developed by Kou [8].

C.2 Pump/Motor Model

The model developed by Kou, describes the relationship between voltage, current, head and flowrate in a pump/motor system with two simple equations. Voltage is assumed to be a function of current and possibly head. The flow rate can then be calculated using the second function relating flow rate, head and voltage.

$$V=f_1(I,H) \tag{C-1}$$

$$m=f_2(V,H) \tag{C-2}$$

For each specific pump, two polynomial functions have to be found using measured data of voltage, current, head and flow rate.

C.2.1 Curve fitting manufacturer's data

The type of data supplied by the manufacturer varies from manufacturer to manufacturer. A good curve fit of the given data is essential for a good simulation. With the two equations introduced above it should be possible to calculate the flow rate of the pump from given data for head, current and voltage. As much data as possible should be used to do the curve fit. If the manufacturer provides data in form of curves, as many data points as possible should be read from it and used for a curve fit. A good curve fit should give good values even for cases that are not specifically stated in the manufacturer's charts or tables. One of the problems for fitting data into only two equations is to find an equation that fits equally well for different heads.

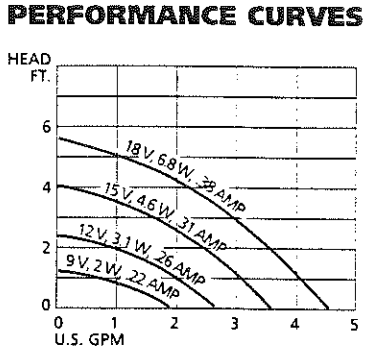

Figure C-1: Manufacturer's Chart Circulating Pump LAING MC-201 DC-N

In the case of the pump used for the experiments, the manufacturer supplied a chart (figure C-1) head over flow rate stating the values for voltage and current for each curve. In this case, voltage and current don't depend on flow rate and head. It was therefore possible to do a curve fit of the given current voltage couples. Only 4 data points are available from the manufacturer. Therefore the highest order equation possible to fit the data with a linear regression is third order. Table C-1 shows the relative errors for each data point and the average errors for all data points for a second and third order polynomial equation.

The third order equation fits the data better than the second order equation although the second order equation also gives reasonable values. The IV characteristic of the pump contains therefore four model parameters:

$$V=f(I)=a_0+a_1 \cdot I+a_2 \cdot I^2\, a_3 \cdot I^3 \qquad (C\text{-}3)$$

This equation determines the operating point of the system as the intersection of the curve with the IV characteristics of the solar panel.

The relationship between flow rate, head, and either voltage or current is given by the manufacturer in form of curves for the four current voltage couples. 60 data points were read from the curve. Using the linear regression function in EES [7], the data was

fitted to polynomial equations of different order. Table C-2 shows the sum of square errors obtained with the different equations. Plots of manufacturer's data and data points calculated with the different curve fits are provided as appendix 2 and 3.

Manufacturer's data		Curve fit	Relative Error
Current	Voltage	Voltage	
Voltage=-1.5982E+01+146.8195*Current-1.5105E+02*Current^2			
0.22	9	9.00747	8.3E-04
0.26	12	11.98009	-16.6E-04
0.31	15	15.01614	10.76E-04
0.38	18	17.99779	-1.2E-04
		Sum of Squares	4.6E-06
		Standard Deviation	**0.00107**
Voltage=-1.9672E+01+185.6548·Current-2.8423E+02·Current^2+148.8095·Current^3			
0.22	9	8.99985	-1.7E-05
0.26	12	11.99978	-1.8E-05
0.31	15	14.99967	-2.2E-05
0.38	18	17.99949	-2.8E-05
		Sum of Squares	1.9E-09
		Standard Deviation	**0.0000216**

Table C-1: Error Calculation: Curve Fit of the IV Characteristic of the Pump with Manufacturer's Data

Order of GPM=f(V,H)	SSQ
2nd	4.219
2nd with cross terms	1.119
3rd	4.081
3rd with cross terms	0.2485
4th	80267
4th with cross terms	30.62

Table C-2 : Sum of Square Errors of Curve Fit of Manufacturer's Data GPM=F(V,H)

The best fitting function is therefore a third order equation with crossterms. See attachments for plots of the manufacturer's data and curves calculated with different order curve fits. The function used in the simulations with manufacturer's data is of the form

$GPM=b_0+b_1\cdot Voltage+b_2\cdot Voltage^2+b_3\cdot Voltage^3+b_4\cdot Head+b_5\cdot Head^2+b_6\cdot Head^3+ b_7\cdot Voltage\cdot Head+b_8\cdot Voltage\cdot Head^2+b_9\cdot Voltage^2\cdot Head+b_{10}\cdot Voltage^2\cdot Head^2$

	Parameter	Value
$V=a_0+a_1*I+a_2*I^2+a_3*I^3$	a_0	-19.672
	a_1	185.6548
	a_2	-284.23
	a_3	148.8095
$GPM=b_0+b_1\cdot Voltage+b_2\cdot Voltage^2+b_3\cdot Voltage^3+b_4\cdot Head+b_5\cdot Head^2+b_6\cdot Head^3+b_7\cdot Voltage\cdot Head+b_8\cdot Voltage\cdot Head^2+b_9\cdot Voltage^2\cdot Head+b_{10}\cdot Voltage^2\cdot Head^2$	b_0	-1.7005
	b_1	0.6533345
	b_2	-0.039378
	b_3	0.00125198
	b_4	-4.1894
	b_5	-1.7646
	b_6	-0.026979
	b_7	0.5791779
	b_8	0.1702965
	b_9	-0.021406
	b_{10}	-0.0036076

Table C-3: Model Parameters for the pump/motor combination obtained through a Curve Fit of Manufacturer's Data

The parameters for the pump motor combination fitted from manufacturer's data is shown in table C-3.

C.3 Hydraulic System and Static and Dynamic Head

The total head of a hydraulic system generally consists of a static head and a dynamic head. The static head is the vertical height between the water level and the point of free discharge. Because of the friction in the pipes, there is a dynamic head that depends on the flow rate and the pipe diameter.

In a solar system, it is especially important to keep the dynamic head small because it reduces the energy consumption of the system and therefore only a smaller PV array can meet the same water needs. If the pressure loss due to friction is small enough to be neglected, the dynamic head becomes zero and the total head is therefore constant if the water level is constant.

D Direct-Coupled Systems

D.1 Introduction

PV pumping systems can be a very efficient way to use solar energy because the times of greatest water need, for example for irrigation in summer coincide with the time of greatest availability of solar energy. Another application for direct-coupled pumping systems is the pump in a solar domestic hot water system. The PV panel would not only provide the energy for the pump but also be the controller that allows the pump to run only when there is enough solar radiation and vary the flow rate with varying radiation levels. In this application, the need for pumping power coincides well with the availability of solar energy.

In direct-coupled PV pumping systems, a DC motor is directly connected to the PV panel. There is no storage battery or controller of any kind. Direct-coupled systems are especially well suited for water pumping systems for irrigation. Water can be stored in a tank and can be used at night or on cloudy days, eliminating the need for and cost of battery storage.

D.2 Operating Point

The operating point of a direct-coupled pumping system is at the intersection of the current -voltage characteristics of PV panel and motor.

Operating current and voltage of the system therefore vary with radiation, temperature, and possibly pump head. Figure D-1 shows the I-V-curve of the LAING MC-201 DC-N pump having a threshold of 9V at a head of 1.5 feet. Also shown is the IV characteristic for the SOLAREX MSX-5L module based on manufacturer's information. At a radiation level of 1000 W/m^2 the two curves have an intersection at about 13V and 0.25A. At 750 W/m^2, the operating point is at significantly lower voltage and current. At 500 W/m^2 however, there is no intersection, which means that the motor wouldn't work at all.

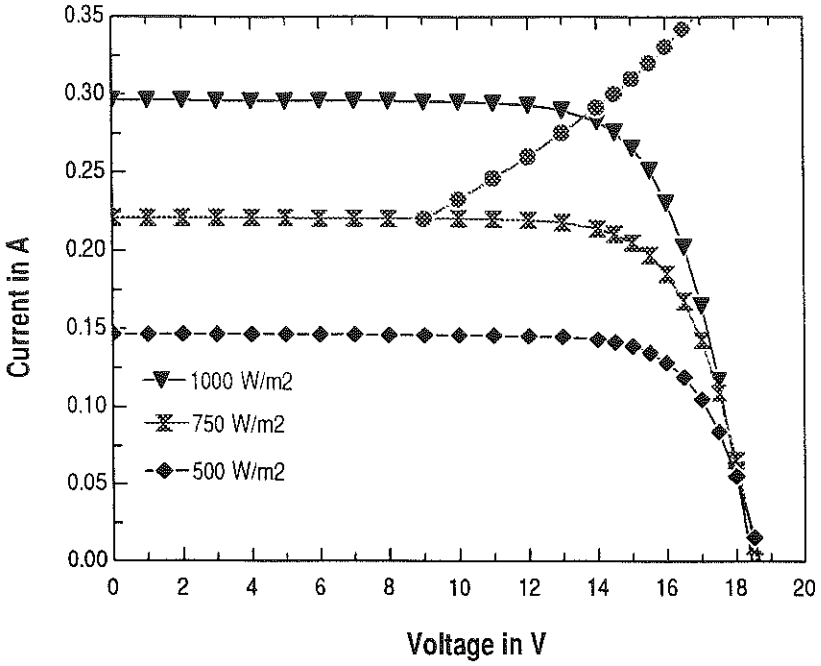

Figure D-1: Operating point of a direct coupled PV pumping system at different radiation levels.

With increasing radiation during the day both the current and voltage of a direct coupled PV pumping system increase. For a system with a maximum power point tracker that always works at the maximum power point of the IV curve of the PV cell, the voltage would stay nearly constant while the current and therefore the power increases. The system that is shown in Figure D-1 does not work at the maximum power points. Because of the shape of the IV characteristic of the pump/motor, the system would work near the maximum power point only at high radiation levels. At lower radiation levels the power output is significantly lower than the maximum possible power that would be reached at the maximum power point.

E Experiments

E.1 PV Panel

The PV panel is mounted horizontally on a wooden stand that allows air to circulate behind the panel. The panel is directly coupled to a pump. There are two PV panels that can be used either separately or connected in series or parallel. The two PV panels are a SOLAREX MSX-5L and a SIEMENS SM6. Table E-1 shows the technical data of both panels as specified by the manufacturers.

	SOLAREX MSX-5L	*SIEMENS SM6*
Max Power, Watts	4.5	6
Voltage at max power point, Volts	16.8	15.0
Current at max power point, Amps	0.27	0.39
Open circuit voltage, Volts	20.6	19.5
Short circuit current, Amps	0.29	0.42
Temperature coefficient of voltage, %/K	-0.3883	-0.36
Temperature coefficient of current, %/K	0.065	0.04
Number of cells in series	36	33
Radiation at reference conditions, W/m^2	1000	1000
Cell temperature at reference conditions, °C	25	25
Length of one cell, mm	19	30
Width of one cell, mm	57	58.3

Table E-1: Manufacturer's data for the PV panels used

The panels are mounted horizontally to be able to use global radiation data measured on a horizontal surface for the predictions. Also no ground reflectance has to be taken into account. For tilted PV panels the radiation would have to be measured with a tilted

pyranometer or calculated from horizontal data which would introduce many more variables into the problem like ground reflectance and ratio of beam and diffuse radiation.

E.2 Hydraulic System

The pump draws water out of a container through a flowmeter and a flexible hose that can be adjusted in height to create different heads. The water is then caught by a funnel and led back to the container. This is shown in Figure E-1. The hose is arranged in a continuously mounting spiral to create a steady flow. The static head of the system is the distance between the water level in the container and the point of free discharge at the top of the spiral.

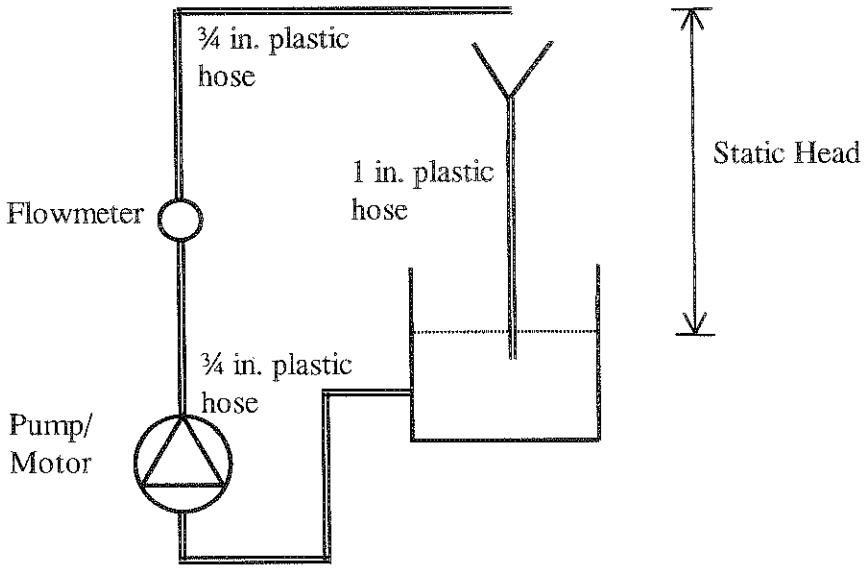

Figure E-1: Hydraulic Setup for the Experiments

E.2.1 Pump

The pump used is a magnetically-coupled DC circulating pump. It is rated at 12V and 3.1 W. It has a NORYL housing and is installed at the lowest point of the hydraulic system to avoid pumping air when the system starts running.

E.2.2 Flowmeter

The flowmeter OMEGA FTB-4607 is installed behind the pump. It is a hall effect turbine flowmeter which puts out a square wave that can be read by the data logging system after adjusting the signal to a square wave between 0 and 5 V.

The maximum pressure drop in the flowmeter is according to the manufacturer's data 3.6 PSI = 0.248184 bars. A pressure drop of 0.24814 bars corresponds to an additional head of 2.5299 m. This maximum pressure drop is reached at the maximum flow rate of 20 GPM. The pressure drop decreases with decreasing flow rate following a quadratic law that is assumed to be of the following form:

$$\Delta H = a^* m^2 + b \qquad \text{(E-1)}$$

The head loss at the flow rates at which the system is going to operate is therefore much lower. Two points are known on the curve: at maximum and at zero flow rate which allows to calculate the parameters a and b in the equation. The head loss is then given as a function of flow rate by

$$\Delta H = 0.0004414\ m^2 \qquad \text{(E-2)}$$

With

ΔH – head loss in the flowmeter in m

m – flow rate in l/min

Figure E-2 shows the head loss due to the flowmeter for different flow rates.

E.2.3 Piping

Plastic hose is used as piping to be able to change the static head of the system easily. A diameter of ¾ in. was chosen to minimize the dynamic head. The diameter of the

hose that is used to guide the water from the funnel back into the container is slightly larger to encure that the water flows back easily. There are no 90-degree elbows in the system. The pressure loss in the hose is considered to be approximately the same as in a straight hose of the same length. The hose is 3.2m long from the container to the point of free discharge.

The Reynolds number for flow in a pipe is defined by

$$\mathrm{Re} = \frac{v \cdot d \cdot \rho}{\mu} \qquad \text{(E-3)}$$

with

v – velocity of fluid in m/s

d – diameter of the pipe

μ - viscosity of water in Ns/m^2

ρ - density of water in kg/m^3

As the flow rate varies the Reynolds number also changes. The friction factor f for different flow rates can be read from the Moody-chart [12]. The head loss is then given by

$$h = f \frac{L}{d} \frac{v^2}{2g} \qquad \text{(E-4)}$$

with

h – head loss of the system

L – length of the pipe

g – gravitational constant

The head loss due to friction in the pipes is indicated in Figure E-2 as a function of flow rate. For low Reynolds numbers the flow is laminar and the friction factor can be calculated with f=64/Re. For high Reynolds numbers the flow turns turbulent and the friction factor has to be read from the Moody chart knowing the roughness factor of the pipe. For this calculations the plastic hose used was assumed to be perfectly smooth. The water was assumed to be at 20°C. The temperature affects the density and the viscosity of water but the influence was found to be insignificant for the value of the head loss in the pipes. The transitional range between laminar and turbulent flow where the friction factor can not be read exactly is indicated in the chart with a dashed line.

pipes. The transitional range between laminar and turbulent flow where the friction factor can not be read exactly is indicated in the chart with a dashed line.

E.2.4 Total Pressure Drop of the Hydraulic System

The total pressure drop of the system is the sum of the pressure drop across the flowmeter and the pressure drop due to friction in the pipes. The total head loss as well as the head losses across the flowmeter and in the pipes are shown in Figure E-2 as a function of flow rate.

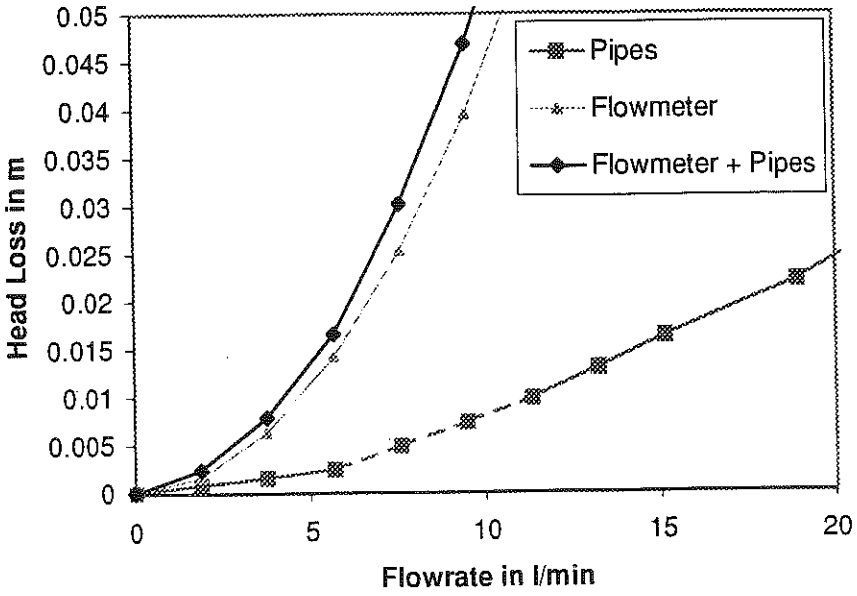

Figure E-2: Head Loss of the System vs. Flow Rate

The head loss due to friction in the pipe is only a few millimeters compared to around 0.6 meters of static head in the system. It can therefore be neglected. On the other hand, the estimated head loss across the flowmeter can not be neglected. It is in the order or a few centimeters and will be taken into account for the predictions.

E.3 Data logging system

To record the experimental data, the KEITHLEY 500 measurement and control system is being used. The system has several input boards that allow reading analog, thermocouple and pulse inputs.

The software used is LABTECH NOTEBOOK. The software allows conveniently acquiring the data, taking averages and saving data to files.

The input boards apply gains to the input signals to be able to use the whole range of 0 to 10 Volts that the data logging system can use as inputs. This increases the resolution that is possible with the 12 bit A/D converter on each input board. For an input that goes up to 10 V the resolution is 2.44 mV.

The Setup of the data logging system is shown in Figure E-3. Appendix 1 shows the setup of the software to acquire data, take averages, and save data to files.

E.3.1 Temperature Measurements

Ambient and cell temperatures of both PV panels are measured. To measure the temperature of the PV cells a thermocouple is glued with aluminum glue onto the back of the panel. The thermocouple is then insulated from the backside. A thermocouple is placed in the shade underneath the PV panel measuring the air temperature near the panel.

The data logging system has an input board called AIM7 that is especially designed for thermocouple inputs. It has a built in cold junction and given the type of thermocouple used the software calculates directly the measured temperature. It applies a gain of 100 and an additional of 1, 2 or 5 depending on the type of thermocouple onto the input signal because the thermocouples have a very low voltage output. The thermocouples used are copper-constantan that have an output of up to 20 mV. This allows a resolution with the 12-bit converter of 9.78 μV which corresponds to 0.18°C.

E.3.2 Flow Measurement

The flowmeter puts out a square wave that has to be adjusted to obtain a square wave between 0 and 5 V as it is necessary for the data logging system. Knowing that the flowmeter gives 75.7 pulses per gallon, the flow rate can be calculated from the frequency counted by the software.

The accuracy of the flowmeter is from 1.1 GPM to 20 GPM ±1.5% of the reading, below 1.1 GPM it's ±2% of reading.

E.3.3 Current and Voltage Measurements

To measure the current a precision resistor of very low resistance (0.1Ω±1%) is connected in series between the PV panel and the pump. The voltage across this resistor is measured with the analog input board of the data logging system. The current can then be calculated with

$$V=IR \tag{E-5}$$

The uncertainty of the resistances causes an uncertainty of also 1% in the current measurement. Other errors that can influence the measurements the A/D conversion the gain applied on the input board or temperature variation of the resistor are very small (in the order of 0.01%) and can be neglected).

The voltage across the PV panel is being measured. Because the data logging system can't take an input greater than 10 V, the voltage is divided by two precision resistors of 1.1 MΩ and 2.15 MΩ respectively. Voltage is measured across the 1.1 MΩ resistor. Both resistors have an accuracy of 1%. The total voltage is calculated with

$$V_{total} = V_1 + V_2 = V_1 + R_2 \cdot \frac{V_{total}}{R_1 + R_2} \tag{E-6}$$

$$V_{total} = \frac{V_1}{\left(1 - \frac{R_2}{R_1 + R_2}\right)} \tag{E-7}$$

An error of +1% in both resistors would result in an error of only 0.15% in voltage.

High resistances are being used to minimize the current going through the voltage measurement branch and not to the motor. At the maximum voltage of around 21V, this current is going to be approximately 6.4 μA which is negligible compared to the operating current of the system.

Measurements are taken every second and averaged over one minute to filter out noise.

E.3.4 Radiation Measurements

The radiation measurements for Madison by the U.S. Department of Commerce National Oceanic and Atmospheric Administration (NOAA) are made next to the experimental setup. The pyranometer used is a Spectrosun Model SR-75 that has a mean uncertainty of 3.6%. Minute data of global radiation on a horizontal surface were downloaded from NOAA to calibrate a second pyranometer that was installed next to next PV panels. Comparison of NOAA data and the own measurements using clear day data at solar elevation angles greater than 45º showed standard deviation of only 0.12%.

The output of the pyranometer was read with thermocouple input board because the pyranometer just like thermocouples puts out very small voltages and the thermocouple input board applies a gain of 100 before converting the analog signal into a digital one.

Instantaneous measurements were taken every minute. During sunny periods the 1-minute interval between instantaneous readings is sufficient. However, the radiation can vary with a frequency greater than one minute. This is a reason why measurements on cloudy parts of the day are fairly inaccurate. Flow rate and also current and voltage measurements are averaged over a minute but radiation measurements are not. If a cloud passes by between two radiation measurements the effect would be recorded only in flow rate, current and voltage but not in radiation. Also when radiation changes voltage, current, and flow rate change rapidly but the true values are only recorded after a full minute of that radiation.

Another problem that occurs with the radiation measurements is the incidence angle of the sun. The reflection of the light off the hemispheric dome of the pyranometer is certainly very different than that off a flat PV panel. The panel is the horizontal so that the panel incidence angles are very small early in the morning and late in the afternoon.

E.3.5 Head Measurements

The static head of the system was measured with a tape measure. The uncertainty of this measurement is about ± 2%.

Small amounts of water evaporated during the measurements. The water level in the

container was filled up occasionally to replace the evaporated water. The effect of the slightly varying head during the measurements has been neglected for the predictions.

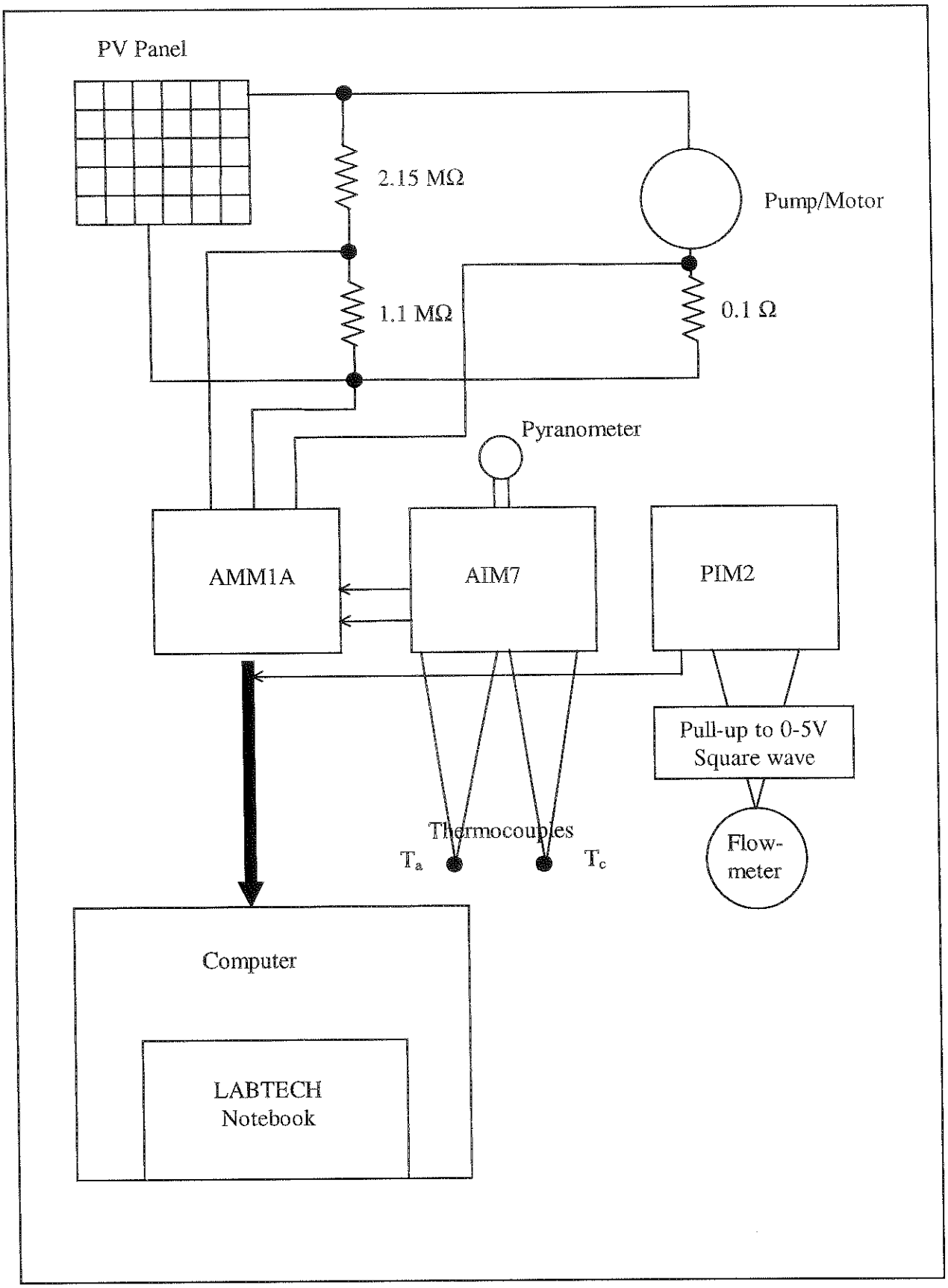

Figure E-3: Data Logging Setup

F Simulations with EES

F.1 EES

Predictions of the performance of the systems have been made using EES [7]. EES stands for Engineering Equation Solver and is a program capable of simultaneously solving sets of non-linear algebraic equations.

The equations for the PV and the pump/motor model were solved for each minute of the experiment. Tables of measured minute by minute data of radiation and cell temperature as well as the measured static head that is assumed to be constant were put into the program and voltage, current and flow rate calculated. An example of an EES program that calculates the performance of the PV pumping system is provided as appendix 4.

F.2 Models Used

The PV model used is the simplified model for crystalline cells with 4 model parameters (equation (B-3)). Manufacturer's data of 3 measured data points as well as measured temperature coefficients of current and voltage were needed to calculate the IV characteristics of the PV module at reference conditions. Equations (B-10) through (B-13) were used to calculate the model parameters at the radiation and cell temperature that was measured during the experiment.

The model for motor and pump has been used to curve fit 2 polynomial equations to the given data from the manufacturer. In the case of the pump used for the experiments, the voltage depends only on current and not on the head. The second equation relates the flow rate with voltage and head.

F.3 Propagation of Errors in the Calculations

F.3.1 Effect on Flow Rate

All performance predictions are based on measurements of three values: the solar radiation, the cell temperature and the head of the hydraulic system. To analyze the

effects of errors in those measurements on the final result (the flow rate), the variation in flow rate was calculated for small changes in those three parameters. Three plots that are attached (appendices 6-7) show this for an assumed error of +2% varying one parameter at a time and for three different values of the other two parameters.

The relative errors in flow rate obtained are considerably larger for low flow rates, which occur at low radiation levels as well as large heads. Flow rate increases with increasing radiation. At radiation levels near the starting point for the particular head the relative errors are especially big becoming infinite at the point where the pump wouldn't work at all but because of the error the radiation limit is reached and the calculated flow rate is greater than zero. Errors at higher radiation levels are around 2%.

The same effect is observed for increasing heads. Larger values for the head of the system lead to an underprediction of flow rate. Near the point where the head becomes too big for the pump to create a flow rate greater than zero, the relative errors become very large. At lower heads and reasonably high radiation levels the errors are smaller than –2%. Errors in radiation and head have to be looked at at the same time as for low radiation levels already smaller heads are close to the operating limit of the pump and errors in head have a significant influence on flow rate calculations.

Generally the flow rate decreases with increasing cell temperature. The cell temperature affects the IV curve of the PV cells. The open circuit voltage decreases and the short circuit current increases slightly with increasing cell temperature. However, a figure that is provided as appendix 7, shows that for a radiation level of 600 W/m^2 the flow rate has a maximum for cell temperatures around 318 K. This effect may be caused by the shape of the IV characteristic of the pump that fixes the operating point of the system for this radiation level at low voltages where the power output of the PV panel increases slightly with increasing cell temperature because of the slightly higher short circuit current. At higher temperatures the effect of cell temperature on the open circuit voltage becomes more important than the increased short circuit current and the flow rate increases.

Errors become important for cases with low flow rate, i.e. for low radiation, large heads, and with increasing cell temperature which causes also low flow rates.

Predictions obtained for low flow rates may have significant errors and should not be used for comparison with experimental data. Only predictions with an error smaller than 5% have been used to make accurate comparisons. The value for the lowest flow rate that gives accurate predictions depends on the radiation, the head, and the cell temperature.

F.3.2 Effect on Power

To study the effect of errors in the measurements of radiation and cell temperature on power, those parameters are varied by 2% for different values of voltage (see appendices 9 and 10). For low voltages the effect of errors in the radiation measurement on the calculated power is around +2% for all radiation levels. Near the maximum power point the errors go down slightly depending on the radiation levels. The largest errors are at low radiation levels. Around the maximum power point they are always smaller or equal to 2%. At high voltages, errors in solar radiation become extremely important. A possible explaination for this behavior is that the effect of errors in radiation is on voltage rather than current. Therefore the effect is not visible for low voltages where the current stays nearly constant.

The effect of errors in cell temperature measurements is very small for low voltages (+0.3%), becomes around zero for the maximum power point, and goes to high negative values for high voltages.

G Comparison of Experimental Results with EES Simulation

Measurements of the flow rate pumped by the system using either the SOLAREX module or the SIEMENS module were each made at two different pump heads. The measurements are compared with predictions for each case that were calculated with the model using manufacturer's data for both the PV panel and the pump motor combination. Plots of flow rate and radiation over time are in appendix 10 and 11.

All measurements show that the system starts working at a considerably lower radiation level than predicted and performs less efficiently than predicted at high radiation levels. The relative error in flow rate is between 20 and 40% for high radiation levels and becomes infinite for low radiation levels when predictions are zero, but the system actually pumps water. As an example figure G-1 shows those curves for the SIEMENS module at 55.8 cm head. Plots of tests at different heads and with the SOLAREX module are

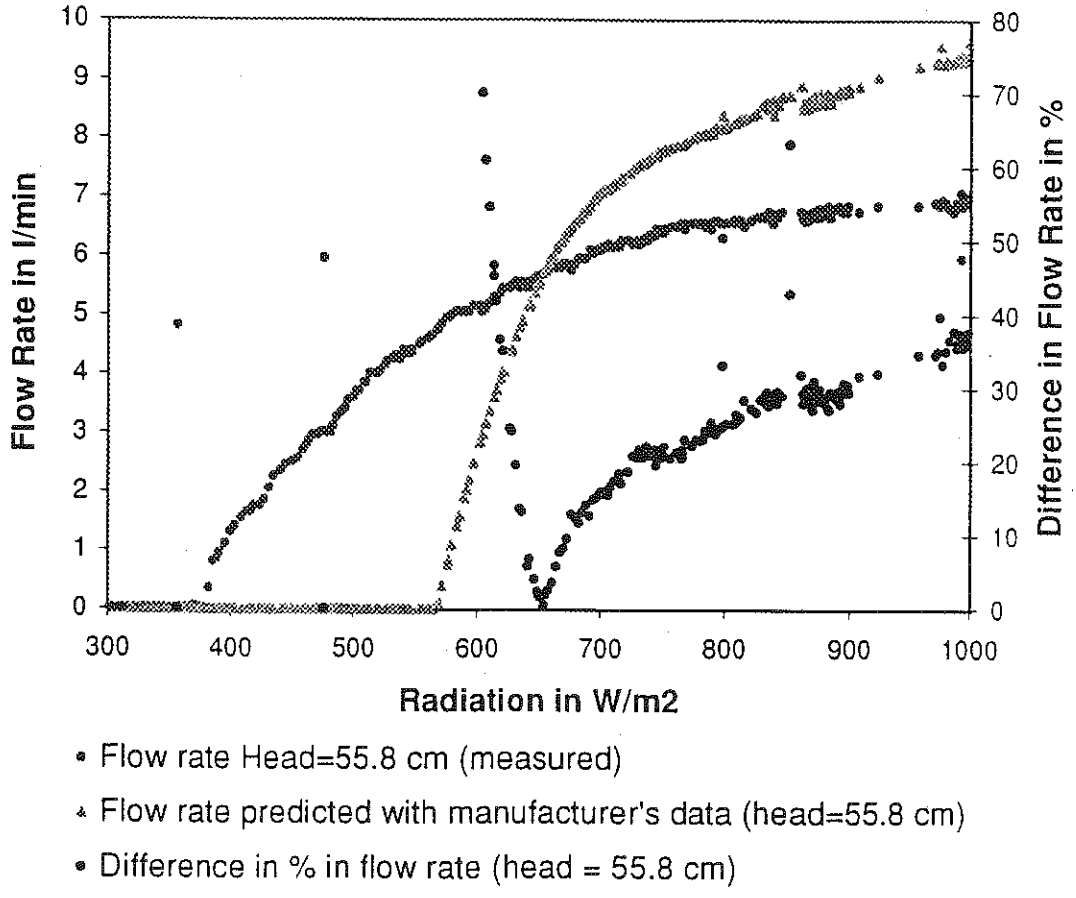

Figure G-1: Measured and Predicted Flow Rate and Difference in % (SIEMENS SM-6)

provided as appendix 12 and 13. The second test of the SIEMENS module with 66 cm head was conducted on a slightly cloudier day which may have led to the strange shape of the curve that suggests that for certain radiation levels, higher radiation results in a lower flow rate. But the general observation and the relative errors are similar to those for the test at a head of 55.8 cm. The tests of the SOLAREX[1] module were conducted on days when the radiation never reached the radiation levels at which predicted flow rates are higher than the measured ones. This critical radiation level seems to be higher for the SOLAREX module which seems reasonable knowing that the SOLAREX module has a lower rated power output than the SIEMENS module. The general prediction errors seem to be very similar for both panels.

By multiplying measured voltage and current, the power output of the system can be calculated. It can then be compared with the predicted power that is determined by the PV

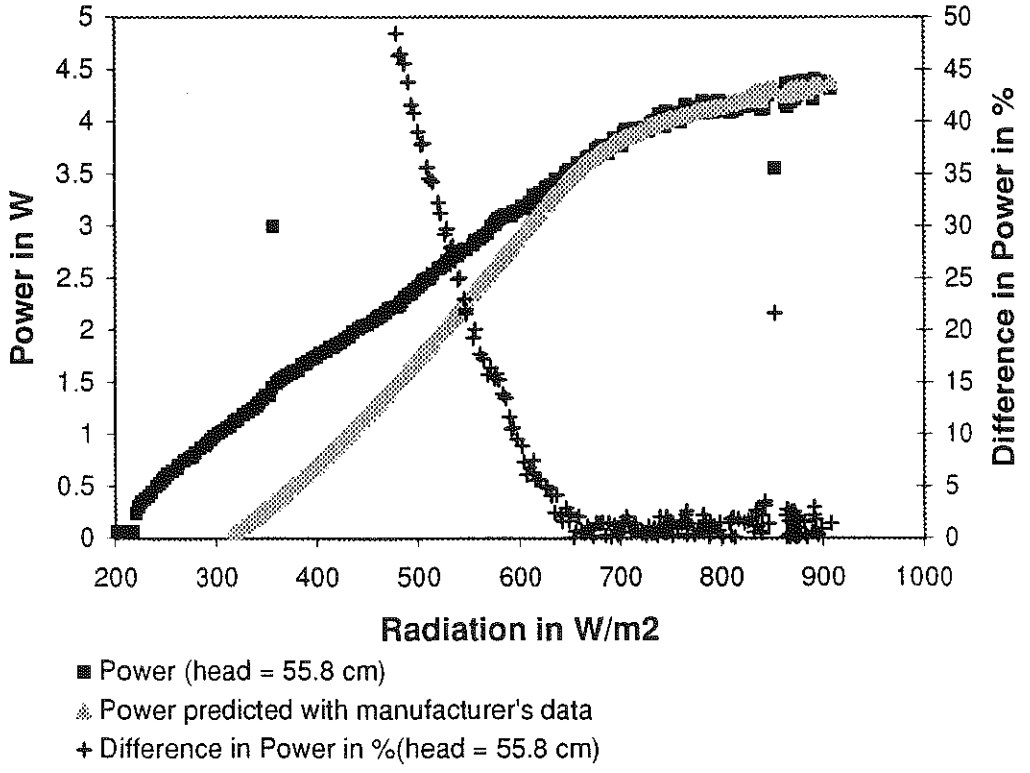

Figure G-2: Measurements and Predictions of the Power Output (SIEMENS module, 55.8 cm head)

[1] For the predictions with manufacturer's data the testing data of the actual panel has been used. See chapter H.1.1 for more information.

model and the IV characteristics of the pump. In this manner, prediction errors caused by a bad curve fit or bad manufacturer's data concerning the flow rate are eliminated from the consideration. Figure G-2 shows the measured and predicted power output as an example again for the SIEMENS module at a head of 55.8 cm. Figure 15 in the appendix is a plot of both tests with the SIEMENS module that shows that the power output is independent of the head of the system. Differences in power output are very small between the two tests. The difference in power between predictions and measurements is very big for low radiation levels and goes down to less 5% for high radiation levels.

Tests of the SOLAREX module showed that the power output varies slightly with the head of the system. Also there is a there are two lines of data that are correspond to measurements in the morning and in the afternoon. This behavior could be an effect of temperature that was different in the morning than in the afternoon. The temperature effect could also explain the different power outputs for different heads because the tests were conducted on different days.

To analyze whether the discrepancies between the calculations and measurements are caused by errors in the model or the manufacturer's data, the models have to be looked at separately.

G.1 Validation of the Predicted Power Output of the System

G.1.1 PV Model

In the original PV model, manufacturer's measurements are used to calculate the model parameters. The accuracy of those measurements as stated by the manufacturers are 10% of power for SIEMENS and 5% of power for SOLAREX testing data of the outgoing panel. SIEMENS data are catalog data. SOLAREX catalog data may vary considerably more. See chapter G.1.1.1 for more details on this topic.

To verify the manufacturer's data, two methods have been used:

1.) Read the three data points usually provided by the manufacturer's off own measurements and use the conditions during the measurements as reference conditions for the model

2.) find the model parameters that best fit the model with a least square curve fit using measured data of current, voltage, radiation and cell temperature.

G.1.1.1 SOLAREX Panel Testing Data

All SOLAREX modules are tested by the manufacturer and the measured parameters are stated on the back of each panel. The panel that was used for the experiments had been found to perform better than indicated in the catalog. The peak power produced at standard test conditions was 4.8W. This value is 5.8% above the average catalog data of 4.536W. Figure (G-2) shows the IV characteristics of the panel that have been calculated

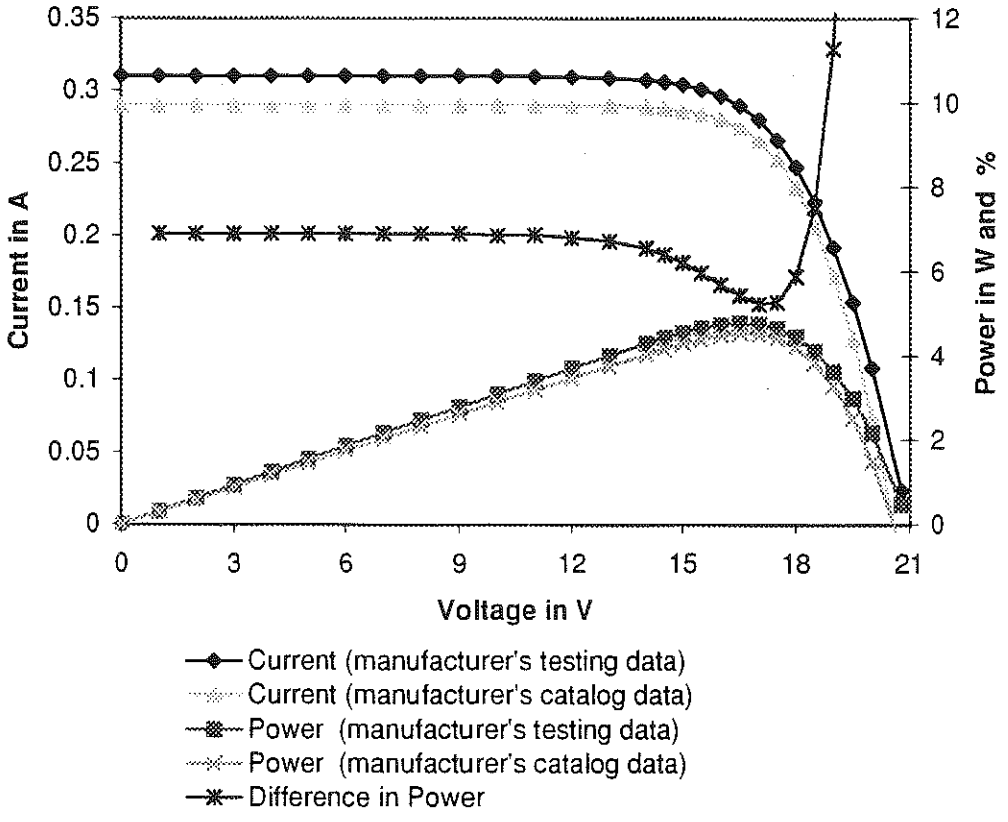

Figure G-3: IV Characteristics of the SOLAREX panel calculated from manufacturer's catalog data and testing data of the actual panel

with EES using the manufacturer's data stated in the catalog and on the back of the panel as well as the difference in power found for each point of the curves. The difference in power is smallest around the maximum power point, about constant around 6.8% for low voltages, and becomes very large for very high voltages near the open circuit voltage.

This fairly large difference in power affects considerably prediction made on the basis of catalog data. Nevertheless, for the following comparisons, the testing data on the actual panel was used.

G.1.1.2 Cell Temperature and Heat Loss Coefficient

The reference cell temperature in the model seems to have a not negligible influence on the quality of predictions at different radiation levels. First measurements with the thermocouple glued onto the back of the panel but not insulated from the back led to calculated IV curves that were different from the measured curves.

	SIEMENS SM6	SOLAREX MSX-5Lite
Radiation in W/m^2	831	828
Measured Cell Temperature in °C	33.2	35.1
Measured Ambient Temperature in °C	21	22
'measured' Heat Loss Coefficient $U_L=\tau\alpha*G/(T_c-T_a)$ in $W/(m^2*K)$	61.303	56.885
Calculated Cell Temperature Using 'measured' U_L	33.2	35.1
Calculated Cell Temperature Using Standard U_L	48.01	48.91

Table G-1: Cell Temperatures and Heat Loss Coefficients

In the PV model, the cell temperature is calculated from the ambient temperature using an energy balance. The heat loss coefficient must be known for this calculation. It coefficient is normally estimated using the following equation [4]:

$$\frac{\tau\alpha}{U_L} = \frac{\left(T_{c,NOCT} - T_a\right)}{G_{T,NOCT}} \qquad \text{(G-1)}$$

The nominal operating cell temperature (NOCT) has to be measured at 20°C ambient temperature, a radiation level of 800 W/m^2, a wind speed of 1 m/s, and no load (η=0). Those conditions couldn't be reproduced in the experiments but measurements at similar conditions could give a good idea of a reasonable value of the heat loss coefficient.

For the initial simulations, a standard value of 46°C for the nominal operating cell temperature was used which leads to a value of 0.0325 for $\tau\alpha/U_L$. Measurements at conditions similar to the nominal operating conditions with a solar radiation of just above 800 W/m^2 and an ambient temperature around 20°C but with considerably higher wind velocities gave the results stated in table H-1. Cell temperatures have than been calculated for no load operation (η=0).

The heat loss coefficients calculated from data using equation (G-1) are considerably different from the standard values used in the early simulations. This is very likely due to the higher wind speed during the experiments. Incorrect values for the heat loss coefficients influence the curves mostly at high voltages because the temperature coefficient of voltage is a lot higher than the temperature coefficient of current. The open circuit voltage decreases significantly more with increasing temperature than the short circuit current increases.

In an environment with varying wind speed it is better to use measured data for the cell temperature than to calculate it using a constant heat loss coefficient. For the simulation of the whole water pumping system, the influence of the heat loss coefficient is very low because the system operates mostly at operating points with voltages lower than the maximum power point where the temperature influence is very small. Nevertheless, for all future calculations the measured cell temperatures were used which takes out the problem of knowing a reasonable heat loss coefficient for the actual conditions of the experiment.

G.1.1.3 Measurements of the IV Curve

To validate the PV model and to verify the model parameters, measurements of the IV curve have been made. A variable resistor of 0 to 900Ω replaced the pump in this experiment. The same electronic circuit as for the other experiments was used to register current and voltage with the data logging system.

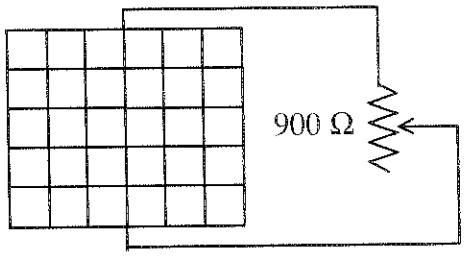

Figure G-4: Setup for IV Curve Measurements

The variable resistor allows measurement of most points on the IV curve. A low resistance puts out low voltage and high current and a high resistance high voltage and low current. Leaving the circuit open allows to measure the open ciruit voltage and taking the resistor out creates a short circuit and the short circuit current can be measured.

It was not possible to measure multiple IV points at constant radiation. Therefore radiation was measured at the same time as current and voltage. Data points could then be sorted according to the radiation while the measurement was taken. Measurements were taken on a clear day. Therefore there were no rapid changes in radiation due to clouds. Two measured IV curves are shown in figure G-5.

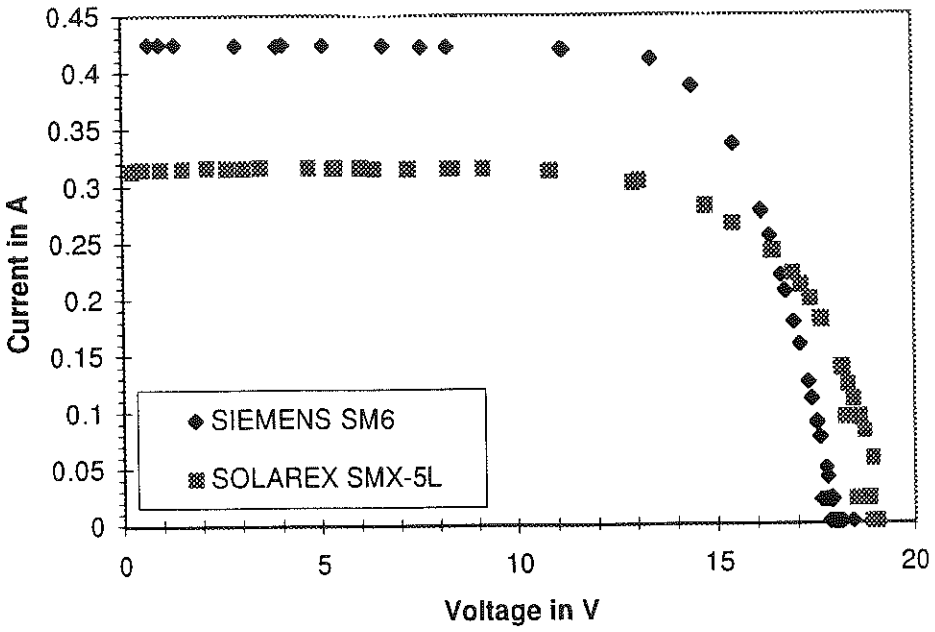

Figure G-5: Measured IV Curves at 1030 W/m^2 and 25°C cell Temperature

G.1.1.4 Curve Fit with Least Squares Method

The parameters of the PV model were calculated using measured data for a least square curve fit. Measurements were made at three different radiation levels: at approximately 340, 540 and 1035 W/m^2 although the radiation for individual points varied slightly form these values. An EES program (see appendix 16) was written that used measured data for voltage, radiation, and cell temperature to calculate the four model parameters I_0, I_L, R_s, and A at reference conditions while minimizing the root mean square of the difference between measured and calculated current.

The root means square (rms) is given by

$$rms = \sqrt{\frac{\sum_{i=1}^{n}\left(I\_measured - I\_calc\right)^2}{n}} \qquad \text{(H-2)}$$

With n - number of measurements

An attempt was made to fit the fifth parameter, the temperature coefficient of voltage to the model, but the values obtained were far off the data measured by the manufacturer. In addition, the measured data did not cover a wide range of cell temperatures. Therefore the manufacturer's data for the temperature coefficient were used for further calculations with curve fitted parameters even though small errors could occur in the model because of an inaccurate measurement of this coefficient. The error introduced by using the manufacturer's temperature coefficients was considered to be negligible.

G.1.2 Comparison of Manufacturer's and Curve Fitted Parameters

Table G-2 summarizes model parameters and characteristic voltages and currents for both modules given by the manufacturer (in the case of the SOLAREX panel the measured data stated on the back of the panel), calculated with the method of least squares from measured data, and data simply read from the measured curves. Parameters calculated with the model are printed in bold.

In the appendix are plots showing the quality of the curve fit for all three cases. The voltages of the IV curve measurements were used to calculate the current obtained with all three sets of parameters. The results are plotted over the corresponding measured current. The quality of the curve fit is summarized by the parameter root mean square (rms).

The model seems to fit the SOLAREX module better than the SIEMENS module. However, for both modules reasonable curve fits can be obtained. For the SOLAREX panel, the model parameters obtained by reading data off a measured curve and taking this condition as reference condition also fits well although the curve fit is best adapted to high voltages which are obtained at radiation levels near the chosen reference conditions. For lower radiation levels this set of parameters is less accurate. But the parameter set read off the measured curve gives at most radiation levels better results as the manufacturer's parameters. For both the manufacturer's set of parameters and the set read off the

measured curve, there are distinguishable lines of data points in the plots that correspond to the three different radiation levels at which measurements were taken. Both sets of parameters work considerably less good for high than for low radiation levels.

For the SIEMENS panel the parameters obtained by reading data off the measured curves gives about equally good results as the manufacturer's data. But both are considerably different than the least square curve fit.

It has to be remarked that in all cases calculated current are equal or higher but never smaller than the measured values. All parameter sets therefore tend to overpredict the power output of the panel.

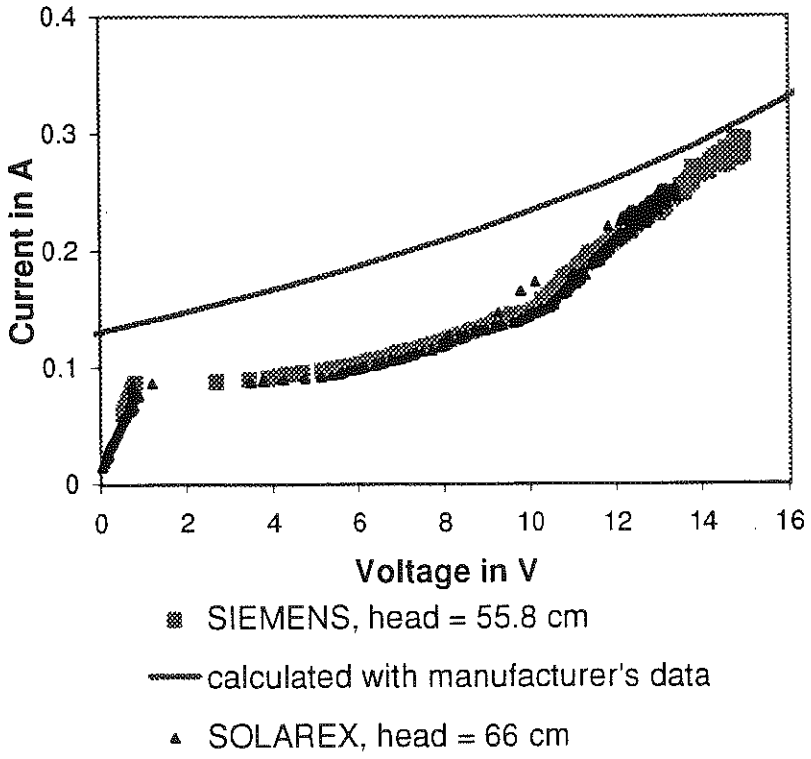

Figure G-6: Operating Points: Experimental Results and Manufacturer's Data

The next step is to look at the influence of the 'corrected' parameters on the predicted power output. This can't be done separately from the IV characteristics of the pump/motor. If for the motor/pump the parameters curve fitted from manufacturer's data is used, the power predictions are even worse than with manufacturer's data for both PV and pump/motor. This is shown as an example for the SOLAREX module in the appendix.

The difference in power is bigger than with just manufacturer's data for all radiation levels except for very high radiation around 900 W/m^2.

G.1.3 Pump Model

Only one of the two equations in the pump/motor model is used to calculate the operating point of the system. Figure H-6 compares the IV characteristics of the motor obtained through a curve fit of the manufacturer's data with the measured operating points

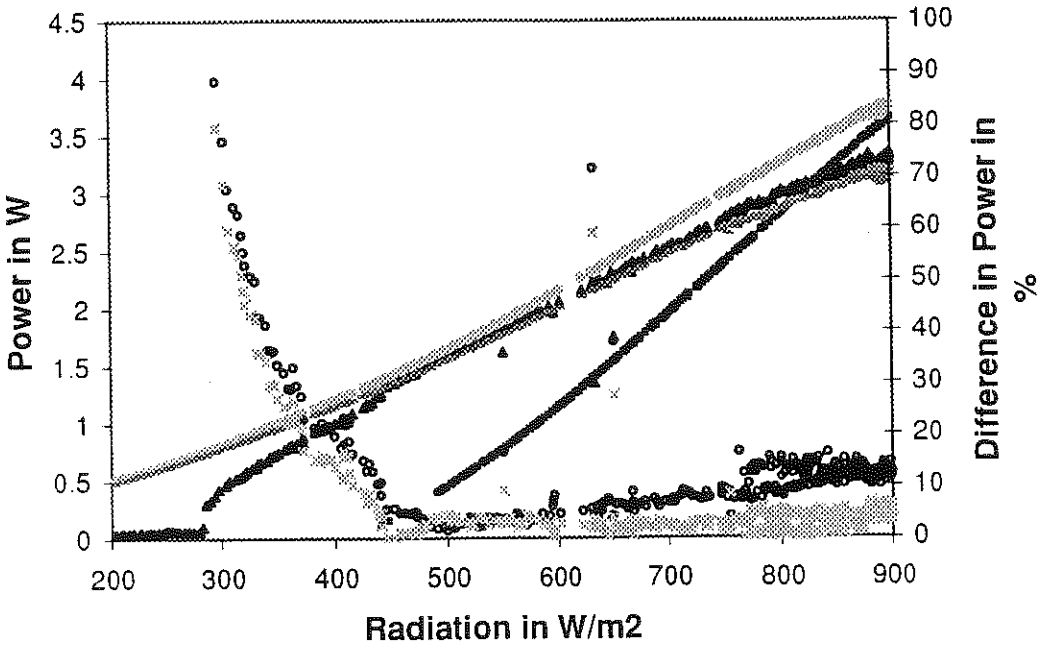

Figure G-7: Corrected IV Characteristic of the Pump

of the system. The operating points of the whole system have to be on the pump/motor characteristic, which is independent of radiation and temperature. The operating points of all tests with different panels and at different heads all fall nearly on one line. This had to

be expected as the same pump/motor combination has been used and the IV characteristics does not depend on the pump head according to manufacturer's information.

This chart shows that for low current (i.e. low radiation levels) the manufacturer's curve predicts lower voltage and therefore lower power output than measured at that current. At higher radiation levels, the errors are smaller or become nearly zero. This matches the differences in power observed during the test for both panels.

A curve fit has been made for the high voltages of the measured operating points. Only the voltages have been used at which the system actually pumped water. At very low voltages (less than 1V) the pump doesn't turn at all, it then starts turning but doesn't pump water until there is enough power to overcome the pump head. A polynomial equation of second order fits well the experimental data (rms = 0.08):

$$V=6.511677+22.22582 \cdot I+22.54495 \cdot I^2 \qquad \text{(G-3)}$$

Using this equation to predict the power output, good results can be obtained even using the manufacturer's parameters for the SIEMENS panel. Predictions are less than 8% off the measured data except for very low radiation levels less than 350 W/m^2. For SOLAREX panel the corrected pump IV characteristics gives good results for lower and medium radiation levels (around 4% difference). At high radiation levels the power output is overpredicted by up to 12%.

G.1.4 Corrected IV Characteristic of the Pump and Least Squares Curve Fit

Using both corrected parameters for the pump IV characteristics and the least squares curve fit gives very good results for the SOLAREX panel. Prediction are equally good for medium raidation levels as without least squares curve fit. For high radiation levels the least squares curve fit results in a very good prediction of also the higher radiation levels (less than 5% difference). The results for the SIEMENS panel are not as good. Predictions are not improved by using the least squares curve fit. For both tested pump heads the calculations underpredict the power output instead of slightly overpredict it without the least squares curve fit.

Figure G-7 shows the effect of the corrected IV characteristic of the pump on the predicted power output. Plots for the other tests are in the appendix (20 and 21).

G.1.5 Incidence Angle Modifier

Theoretically, the short circuit current of a solar cell is directly proportional to the radiation level. Figure G-8 shows the three measured short circuit currents over radiation. They do not lie on a straight line. As already mentioned in chapter E.1.3.4 a reason might be that reflection off the PV panel is higher at high incidence angles. Therefore the radiation that is actually absorbed by the cells is lower than the radiation measured by the pyranometer. To account for these effects, an incidence angle modifier can be used [4].

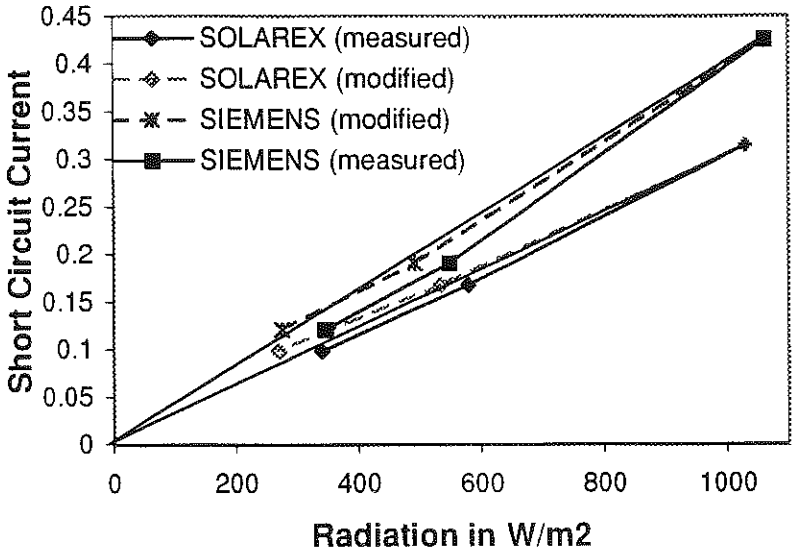

Figure G-8: Measured Short Circuit Current as a Function of Radiation with and without Incidence Angle Modifier

The angle of incidence is smallest at noon and 90° at sunset. The incidence angle modifier $K_{\tau\alpha}$ is defined by

$$K_{\tau\alpha} = \frac{(\tau\alpha)}{(\tau\alpha)_n} = 1 + b_0\left(\frac{1}{\cos\theta} - 1\right) \qquad \text{(G-4)}$$

With t - transmittance of the cover

a - absorptance of the cells

n - at normal incident

Equation (G-4) is valid only for incidence angles smaller than 60º.

The absorptance is assumed to be independent of the incidence angle and therefore does not need to be considered. The angular dependence of the transmittance depends very much on the nature of the cover. The dependence is not known for the covers used in the tested panels. As an estimation a curve showing the transmittance as a function of angle of incidence of a nonabsorbing cover having an index of refraction of 1.526 has been used [4]. The values for the three angles of incidence θ that can be calculated with equation (G-5) knowing the time of the day of the measurement have been read from the curve.

$$\cos\theta_z = \cos\varphi\cdot\cos\delta\cdot\cos\omega+\sin\varphi\cdot\sin\delta \qquad \text{(G–5)}$$

with θ_z - zenith angle (angle between the vertical and the line to the sun)

φ - latitude

δ – declination angle (anglular position of the sun at solar noon)

$$\delta = 23.45\cdot\sin\left(360\frac{284+n}{365}\right) \qquad \text{(G-6)}$$

n - day of the year

ω - hour angle (15°per hour, negative in the morning, positive in the afternoon)

Because the PV panels were installed horizontally the angle of incidence is equal to the zenith angle.

Using the measured values at the short circuit current, the incidence angle modifier coefficient b_0 can be calculated using equation (G-4) using the measurement at very high radiation (more than 1000 W/m^2) as the reference value $(\tau\alpha)_n$:

$$\frac{\frac{(\tau\alpha)_1}{(\tau\alpha)_n}}{\frac{(\tau\alpha)_2}{(\tau\alpha)_n}} = \frac{(\tau\alpha)}{(\tau\alpha)_2} = \frac{1 + b_0\left(\frac{1}{\cos\theta_1} - 1\right)}{+ b_0\left(\frac{1}{\cos\theta_2} - 1\right)} \qquad \text{(G-7)}$$

b_0 was found to be –0.092. Using this coefficient all other transmittances can be calculated if the incidence angle is known. The adjusted radiation is then calculated with

$$S_{adjusted} = (\tau\alpha) S_{measured} \qquad \text{(G-8)}$$

and the results are also shown in Figure (H-8). The absorptance was assumed to be 100%.

For the SIEMENS panel, the two low radiation measurements are much closer to the straight line between the high radiation point and the origin. For the SOLAREX module, the calculated radiation is now a little bit lower than what would be expected knowing that the radiation is proportional to the short circuit current. The reflectance and

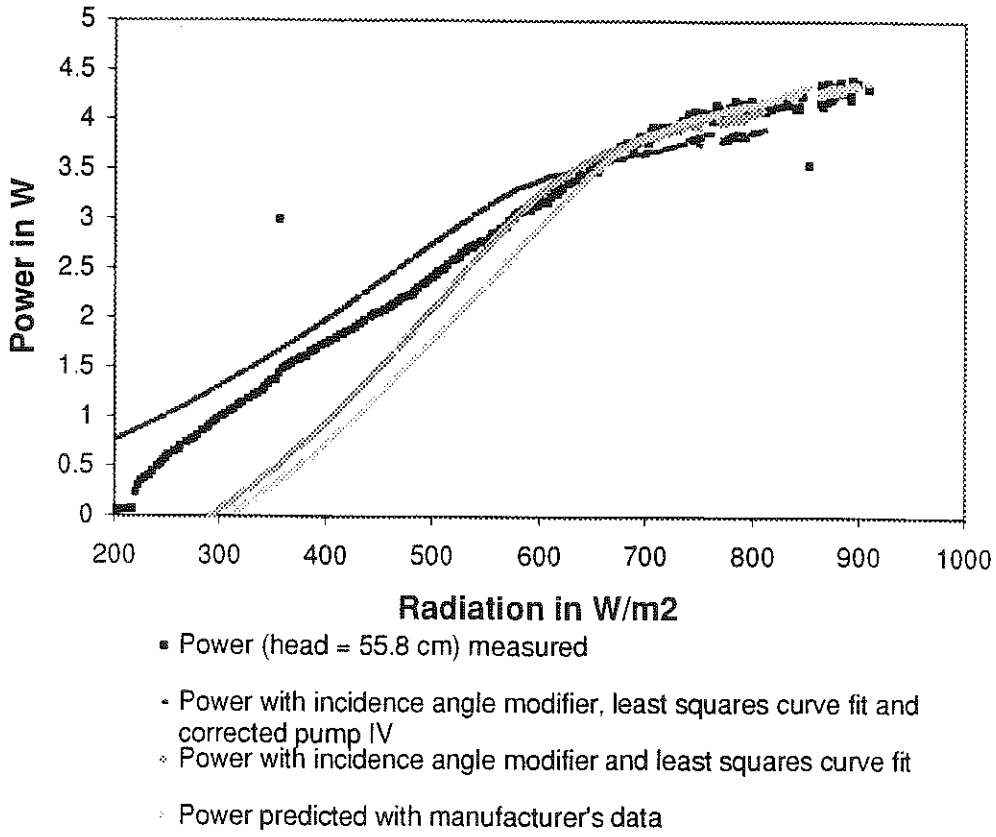

Figure G-9: Predictions with Incidence Angle Modifier(SIEMENS, 55.8 cm head)

therefore also the transmittance of the SOLAREX panel cover seems to depend less on the angle of incidence than the SIEMENS cover. The use of the incidence angle modifier does not seem to give good results for the SOLAREX module. It is obvious that the angle of incidence does not have the same effect on the two different covers because the materials are very different. The SOLAREX panel is covered only with a very thin bonded plastic film, the SIEMENS panel on the other hand has a hard plastic cover.

The radiation levels measured during the IV curve measurements were then adjusted and a new least square curve fit done with the measured data. For the SIEMENS panel a better curve fit was obtained with a root mean square of 0.01427. As expected, the curve fit for the SOLAREX panel was less good than when using measured radiation data with a rms of 0.01179 as opposed to 0.00873 without incidence angle modifier. Plots of the measured over the calculated current are in appendix 22 and 23.

Calculations of the power output of the system using the parameters obtained in this curve fit with incidence angle modifier were made. Not only the changed parameters for the PV model were used but also the measured radiation multiplied with the calculated transmittance depending on the angle of incidence.

Figure G-9 shows the obtained power output compared with measured data and predictions made with manufacturer's data for the SIEMENS panel at 55.8 cm of pump head. The results are slightly better with the incidence angle modifier than without when using manufacturer's data for the pump, especially for low radiation levels. When using the curve fitted equation for the pump the use of the new least squares curve fit for the PV gives better results than with the least squares curve fit with out incidence angle modifier but not better than with manufacturer's data.

For the SOLAREX panel the use of the incidence angle modifier does not give better results. The predicted power is for all radiation levels higher than the measured values. Plots for the SOLAREX panel and the SIEMENS panel at different heads are in the appendix (24-26).

		Manufacturer's data	Least Square Curve Fit	Data Read from Curve	Least Squares Curve Fit with incidence Angle Modifier
SIEMENS	G_{ref}	1000 W/m^2	1000 W/m^2	1032 W/m^2	1000 W/m^2
	T_{cref}	25°C	25°C	43°C	25°C
	I_{Lref}	**0.42**	**0. 3699**	**0.427**	**0.4456**
	I_{0ref}	**1.217E-11**	**4.478e-11**	**1.8e-11**	**4.867e-11**
	R_{sref}	**6.1**	**3.27**	**4.848**	**3.402**
	A_{ref}	**0.8037**	**0.8041**	**0.7577**	**0.8042**
	$V_{oc,ref}$	19.5 V		18.1 V	
	$I_{sc,ref}$	0.42 A		0.427 A	
	$V_{m,ref}$	15 V		14.25 V	
	$I_{m,ref}$	0.39 A		0.394 A	
	$P_{m,ref}$	6 W		5.61 W	
SOLAREX	G_{ref}	1000 W/m^2	1000 W/m^2	1040 W/m^2	1000 W/m^2
	T_{cref}	25°C	**25°C**	43°C	25°C
	I_{Lref}	**0.31**	**0.2988**	**0.317**	**0.3371**
	I_{0ref}	**4.314e-9**	**3.551e-8**	**1.607e-9**	**1.403e-8**
	R_{sref}	**4.604**	**4.071**	**7.713**	**6.321**
	A_{ref}	**1.161**	**1.207**	**1**	**1.157**
	V_{oc}	21 V		19.1V	
	I_{sc}	0.31 A		0.317 A	
	V_m	17 V		14.7322 V	
	I_m	0.28 A		0.2817 A	
	P_m	4.8 W		4.15 W	

Table G-1: Comparison of Parameters for the PV Model

G.1.6 Conclusion

Table H-2 summarizes the different parameter sets obtained for the two PV panel. The biggest influence on the power output predictions has the IV characteristics of the

pump that does not match the manufacturer's data. Even with manufacturer's data for the PV good predictions were obtained for the SIEMENS panel. For the SOLAREX panel the least squares curve fit without incidence angle modifier gives good results.

The SIEMENS panel seems to have far more reflection losses due to high incidence angles early in the morning and late in the afternoon. Adjusting the radiation levels with an incidence angle modifier was attempted. For the SIEMENS panel better results than with a curve fit without incidence angle modifier could be obtained but the results are not satisfactory. Measurements of the characteristics of the covers would have to be made to be able to calculate the transmittance more exactly. Also the incidence angle of one of the

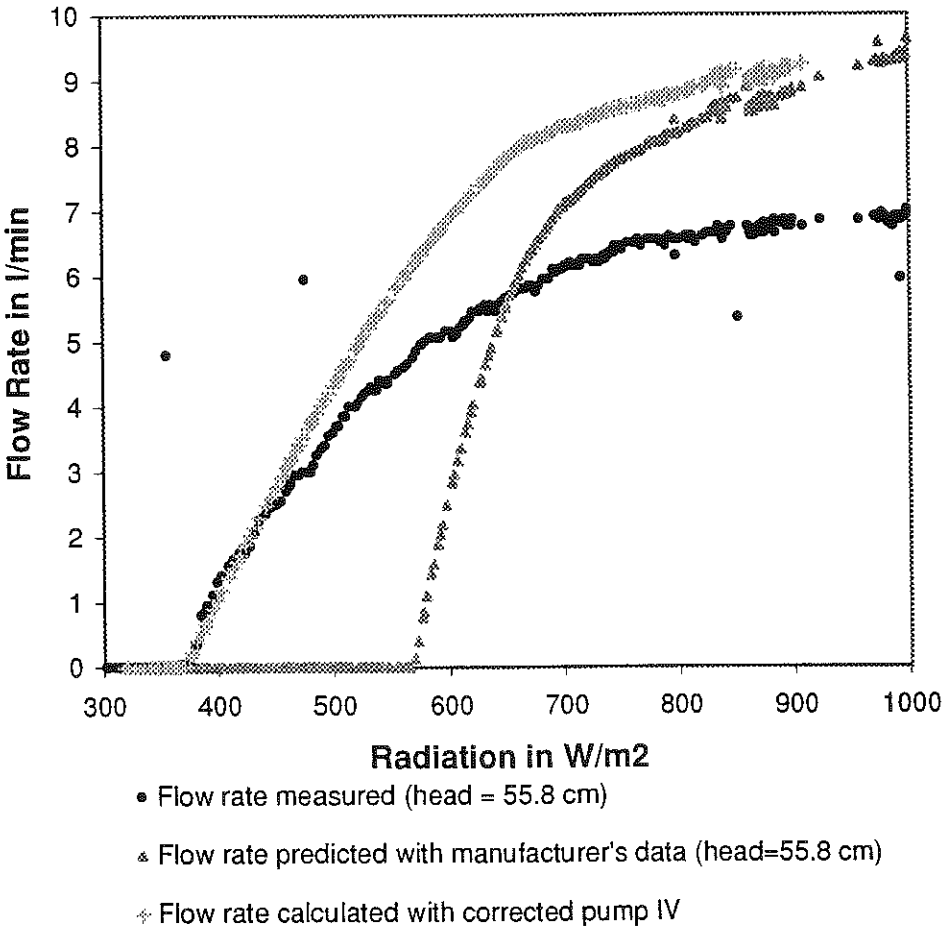

Figure G-10: Predicted Flow Rate with Corrected Pump IV Characteristics

IV curve measurements was around 70°. Therefore equation (H-4) was not valid but was used as estimation. The values obtained for the transmittance at high incidence angles are also only an estimation. Better curve fits of the dependence of the transmittance of the incidence angle would have to be made.

G.2 Validation of the Flow Rate Predictions

In the simulations, the flow rate pumped is calculated as a function of voltage and head. The voltage depends on the operating point of the system. After adjusting the IV characteristics of the pump. Measured and calculated voltages match fairly well. The flow rate calculated with the obtained voltages is shown in Figure G-10. It matches very well at low radiation levels but overpredicts significantly at high radiation levels. Figure H-11

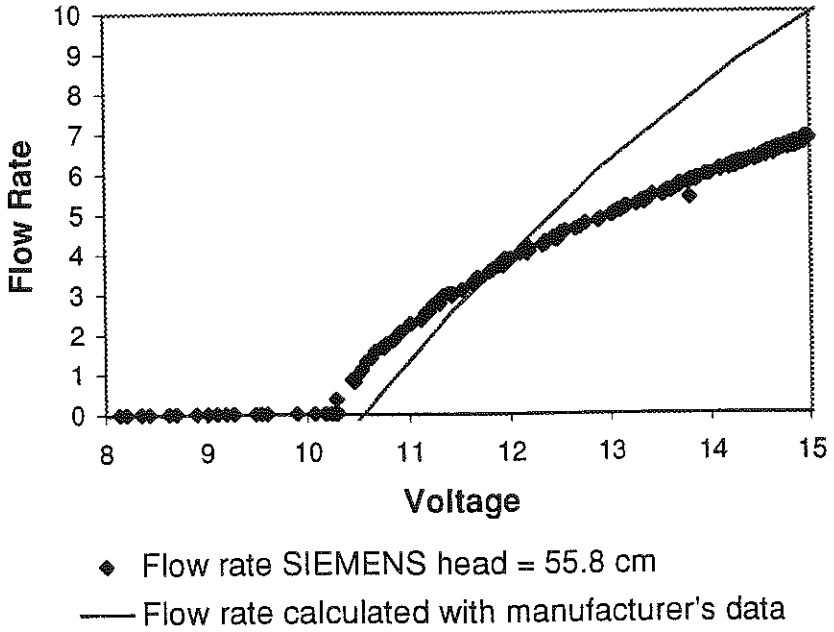

Figure G-11: Flow Rate Equation of the Pump (Measured and Predicted Data)

shows the measured flow rate over the measured voltages as an example for the SIEMENS module at a head of 55.8 cm. This plot explains why the model with the manufacturer's data overpredicts at high radiation levels. Manufacturer's and measured curve match fairly well at low voltages but they are very different at high voltages.

The pumped flow rate depends on the head. Because measurements were made at only two different heads for each panel, it was not possible to do a curve fit like for the manufacturer's data.

Doing a curve fit for a constant head (flow rate only as a function of voltage) obviously gives good results in predicting the flow rate pumped.

H Conclusion and Recommendations

H.1 Conclusions

An experimental setup has been designed that allows measuring the performance of a small-scale direct-coupled PV pumping system. Voltage, current, ambient and cell temperatures and radiation pump head and flow rate were measured at one minute intervals.

Tests have been performed using a DC circulating pump direct-coupled to a PV module. Two different modules were tested.

Predictions of the performance of the system were made using a 4-parameter PV model and two equations as a model for pump and motor curve fitted from manufacturer's data. Predictions were made based on measured radiation and cell temperature for the actual test day.

Comparing the predictions and the measurements showed significant differences between measurements and predictions.

The different models and model parameters have then been compared separately. The difference of the IV characteristics of the motor between manufacturer's and measured data has been found to have the biggest influence on the predictions of the power output of the system.

The PV model works fairly well even with manufacturer's data. A curve fit of the model parameters has been attempted using measured data of the IV curve of the PV panels. For one of the panels the obtained parameters gave better results than the manufacturer's parameters, for the other one the transmittance of the cover over the PV cells seems to depend considerably on the angle of incidence. Adjusting the measured radiation with an incidence angle modifier has been attempted but the results were not satisfactory because of the lack of data on the cover of the panel.

The second equation used to calculate the pumped flow rate from the voltage output of the system also did not match the experimental data. Curve fitting an equation onto the measured values obviously allows predicting the pumped flow rate fairly accurately.

H.2 Recommendations

Some tests have been carried out and results have been obtained. It would have been desirable to test of a large number of different PV modules and pumps from different manufacturers. Also tests at many different heads should be done to validate the model using one equation relating the flow rate to the voltage and the pump head of the system.

The effects of using current, voltage or power to calculate flow rate should be studied. Can the error made by using a badly predicted voltage in the equation determining flow rate be reduced by using current or power instead?

The influence of the nature of the cover over the PV cells on the absorbed radiation will have to be studied to be able to predict the flow rate pumped at high incidence angles. Tests with PV panels at a slope would reduce the amount of data at high incidence angles.

References

[1] ASHRAE Handbook - Fundamentals, American Society of Heating, Refrigerating and Air-Conditioning Engineers, Inc., Atlanta, 1993.

[2] Diarra, M., Diarra, N., Kenna, J.P., McNelis, B., Traore, C., "Development and Application of an Evaluation Methodology for Photovoltaic Pumps: Proposal for a Global Standard", Proceedings 6th Solar Energy Conference, London, 1985.

[3] Derrick, A., Hacker, R.J., Napier, A.P., O'Hea, A.R., "Performance Monitoring of Small-Scale Solar-Powered Pumping Systems", Proceedings Solar World Forum, London, 1982.

[4] Duffie, John A., Beckman, William A., "Solar Engineering of Thermal Processes", John Wiley & Sons, Inc., New York, ²1991.

[5] Eckstein, Jürgen H., "Detailed Modeling of Photovoltaic System Components", M.S. Thesis, Mechanical Engineering, University of Wisconsin – Madison, 1990.

[6] Kenna, J.P., Gillett, W.B., "Solar Water Pumping – A Handbook", I.T.Publications, London, 1985.

[7] Klein, S.A., Alvarado, F.L., "Engineering Equation Solver", Computer Program, Middleton, 1992-1997.

[8] Kou, Qing, "A method for Estimating the Long-Term Performance of Photovoltaic Pumping Systems", M.S. Thesis, Mechanical Engineering, University of Wisconsin – Madison, 1996.

[9] Rauschenbach, H.S., "Solar Cell Array Design Handbook. The Priciples and Technology of Photovoltaic Enefgy Conversion", Van Nostrand Reinhold, New York, 1980.

[10] Stoecker, Wilbert F., Jones, Jerold W., "Refrigeration & Air Conditioning", McGraw-Hill Book Company, Auckland, ²1982.

[11] Townsend, T.U., ""A Method for Estimating the Long-Term Performance of Photovoltaic Systems" M.S. Thesis, Mechanical Engineering, University of Wisconsin – Madison, 1989.

[12] White, Frank M., "Fluid Mechanics", McGraw-Hill Book Company, New York, ²1986.

Appendix

Appendix 1: Setup of Labtech Notebook for the experiments

Appendix 2: Pump manufacturer's data and 3rd and 4th order curve fits

Appendix 3: Pump manufacturer's data and 2nd order curve fits

Appendix 4: EES program that calculates the performance of the PV pumping system from measured radiation and cell temperature

Appendix 5: Effect of a 2% error in radiation on flow rate

Appendix 6: Effect on a 2% error in cell temperature on flow rate

Appendix 7: Effect of a 2% error in static head on flow rate

Appendix 8: Effect of a 2% error in cell temperature on power

Appendix 9: Effect of a 2% error in radiation on power

Appendix 10: Radiation and measured and predicted flow rate at two different pump heads over time (SOLAREX)

Appendix 11: Radiation and measured and predicted flow rate at two different pump heads over time (SIEMENS)

Appendix 12: Flow rate as a function of radiation for two different heads, measurements and predictions with manufacturer's data and difference in % (SIEMENS)

Appendix 13: Flow rate as a function of radiation for two different heads, measurements and predictions with manufacturer's data and difference in % (SOLAREX)

Appendix 14: Measured and predicted power output as a function of radiation at two different pump heads and difference in % (SOLAREX)

Appendix 15: Measured and predicted power output as a function of radiation at two different pump heads and difference in % (SIEMENS)

Appendix 16: EES program for curve fitting measured IV data to the PV model

Appendix 17: Calculated vs. measured current with different sets of parameters without incidence angle modifier (SOLAREX)

Appendix 18: Calculated vs. measured current with different sets of parameters without incidence angle modifier (SIEMENS)

Appendix 19: Measured power and power predicted with manufacturer's data and with least squares curve fit without incidence angle modifier and difference in %(SOLAREX)

Appendix 20: Measured and predicted power with corrected pump IV characteristics only and with corrected pump IV and least squares curve fit without incidence angle modifier and difference in % at 55.8 cm pump head (SIEMENS)

Appendix 21: Measured and predicted power with corrected pump IV characteristics only and with corrected pump IV and least squares curve fit without incidence angle modifier and difference in % at 66 cm pump head (SIEMENS)

Appendix 22: Calculated over measured current for the least squares curve fit with incidence angle modifier (SOLAREX)

Appendix 23: Calculated over measured current for the least squares curve fit with incidence angle modifier (SIEMENS)

Appendix 24: Measured and predicted power with incidence angle modifier, least squares curve fit and with and without corrected pump IV (SOLAREX)

Appendix 25: Measured and predicted power with and without incidence angle modifier, least squares curve fit and corrected pump IV (SIEMENS, head = 66 cm)

Appendix 26: Measured and predicted power with and without incidence angle modifier, least squares curve fit and corrected pump IV (SIEMENS, head = 55.8 cm)

Appendix 27: Measured and predicted flow rate with manufacturer's data, least squares curve fit, corrected pump IV and corrected flow rate equation (SIEMENS)

LABTECH NOTEBOOK Global Setup Checking MODE: Normal

Bl. No.	Block Name	Intfc Dev	Intfc Ch	Block Function	Block Info.	Scale Factor	Offset	Iter	Stg	Stage Information: Duration (sec)	Stage Information: Rate (sec)	Stage Information: Start State	Stage Information: Tr. Ch.	File Name (first)
1	cell T SOLAREX	2	6	Tcpl(T)	Celsius	1.000	0.000	1	1	4.32E+04	1.000	Normal	1	
2	Time			Time	T-O-D			1	1	4.32E+04	60.000	Normal	1	
3	amb. Temp	2	0	Tcpl(T)	Celsius	1.000	0.000	1	1	4.32E+04	1.000	Normal	1	
4	Voltage	0	2	Analog In	+/-10 V	2.955	0.000	1	1	4.32E+04	1.000	Normal	1	
5	Current	0	1	Analog In	+/-0.1 V	10.000	0.000	1	1	4.32E+04	1.000	Normal	1	
6	Power			(10)*(9)	0.000	1.000	0.000	1	1	4.32E+04	60.000	Normal	1	
7	Frequency	3	3	Frequency				1	1	4.32E+04	20.000	Normal	1	
8	Radiation	2	5	Analog In	+/-0.02*	1.000	0.000	1	1	4.32E+04	60.000	Normal	1	rad@.prn
9	Voltage (av)			Blk Av(4)	60.000	1.000	0.000	1	1	4.32E+04	60.000	Normal	1	resu@.prn
10	Current (av)			Blk Av(5)	60.000	1.000	0.000	1	1	4.32E+04	60.000	Normal	1	resu@.prn
11	gpm			(13)	60.000	0.793	0.000	1	1	4.32E+04	60.000	Normal	1	
12	Radiation			(8)	0.000	9.84E+04	0.000	1	1	4.32E+04	60.000	Normal	1	
13	av. Frequency			Blk Av(7)	3.000	1.000	0.000	1	1	4.32E+04	60.000	Normal	1	resu@.prn
14	SOLAREX av.			Blk Av(1)	60.000	1.000	0.000	1	1	4.32E+04	60.000	Normal	1	resu@.prn
15	amb Temp (av)			Blk Av(3)	60.000	1.000	0.000	1	1	4.32E+04	1.000	Normal	1	
16	cell T Siemens	2	14	Tcpl(T)	Celsius	1.000	0.000	1	1	4.32E+04	60.000	Normal	1	resu@.prn
17	SIEMENS (av)			Blk Av(16)	60.000	1.000	0.000	1	1	4.32E+04	60.000	Normal	1	resu@.prn
18	l/m			(11)	60.000	3.785	0.000	1	1	4.32E+04	60.000	Normal	1	

Setup OK

Interface Devices:
  0: AMM1A
  1: AIM8
  2: AIM7
  3: PIM2

Appendix 1: Setup of Labtech Notebook for the experiments

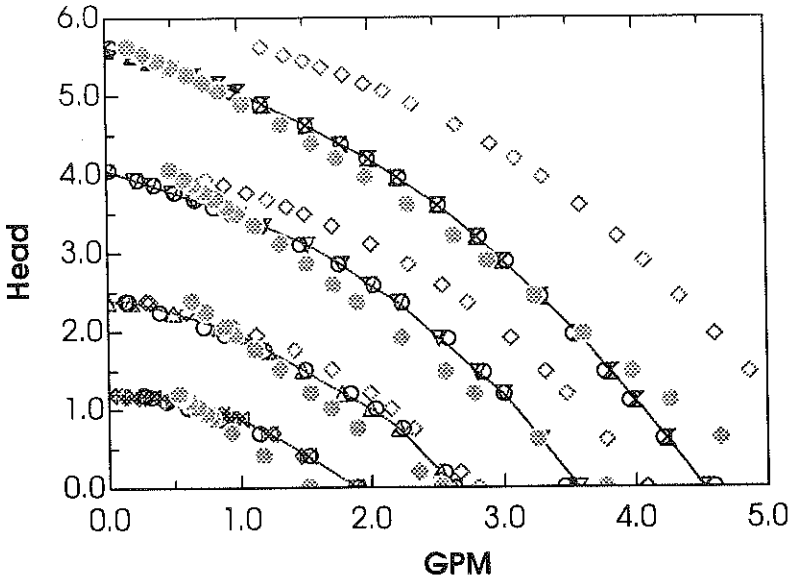

○ 3rd order curve fit with crossterms SSQ=0.2485

◇ 4th order curve fit with crossterms SQQ=30.64

3rd order SQQ=4.081

18V, 0.38A

15V, 0.31A

12V, 0.26A

9V, 0.22A

Appendix 2: Pump manufacturer's data and 3rd and 4th order curve fits

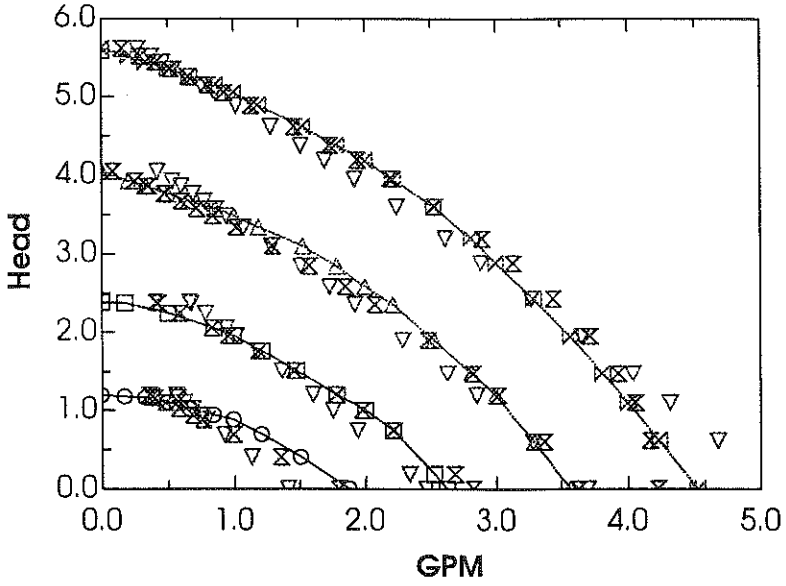

▽ 2nd order curve fit SSQ=4.219

⧖ 2nd order curve fit with cross terms SSQ=1.119

18V, 0.38A

15V, 0.31A

12V, 0.26A

9V, 0.22A

Appendix 3: Pump manufacturer's data and 2nd order curve fits

Appendix 44: EES program that calculates the performance of the PV pumping system from measured radiation and cell temperature


```
Procedure Zero (GPM : Flow)
  If (GPM < 0) Then        Flow := 0        Else        Flow := GPM
EndIf
End Zero

Look up weather data
Rad = Lookup(row, 'modified Radiation')
T_c = 273.1 + Lookup(row, 'T_c')
G_ref = 1000
G = Max(0, Rad)
T_cref = 298.1
Module
crystalline model
Parameters (manufacturer's data)
I_sc = 0.42
V_oc = 19.5
V_m = 15
I_m = 0.39
mue_Voc = -0.0702
mue_Isc = 0.000168
Eq = 1.155          band gap of silicon
Ns = 33             number of cells in series in one module
calculated module parameters at reference conditions
least squares
read from curve
least squares new
least squares with incidence angle modifier
A_ref = 0.8042
```

$I_{0ref} = 4.867 \times 10^{-11}$

$I_{Lref} = 0.4456$

$R_{sref} = 3.402$

Changing of weather conditions

$$I_L = \frac{G}{G_{ref}} \cdot (I_{Lref} + mue_{Isc} \cdot (T_c - T_{cref}))$$

$$I_0 = I_{0ref} \cdot \left[\frac{T_c}{T_{cref}}\right]^3 \cdot \mathbf{exp}\left[Ns \cdot \frac{Eq}{A_{ref}} \cdot \left(1 - \frac{T_{cref}}{T_c}\right)\right]$$

$R_s = R_{sref}$

$$A = A_{ref} \cdot \frac{T_c}{T_{cref}}$$

Equations

$$I = I_L - I_0 \cdot \left[\mathbf{exp}\left(\frac{V + I \cdot R_s}{A}\right) - 1\right]$$

$Power = V \cdot I$

Pump/Motor

Parameters

$head_{static} = 0.66$

$$Head = Head\backslash m \cdot \frac{100}{30.4}$$

$Head\backslash m = head_{static} + head_{loss}$

$head_{loss} = 0.0004414 \cdot Liters^2$

Equations

$V = -19.67 + 185.7 \cdot I - 284.2 \cdot I^2 + 148.8 \cdot I^3$

curve fitted equation

3rd order with cross terms 60 data points table

$$GPM = -1.701 + 0.6533 \cdot V - 0.03938 \cdot V^2 + 0.001252 \cdot V^3 - 4.189 \cdot Head - 1.765 \cdot Head^2 - 0.02698 \cdot Head^3 + 0.5792 \cdot V \cdot Head + 0.1703 \cdot V \cdot Head^2 - 0.02141 \cdot V^2 \cdot Head - 0.003608 \cdot V^2 \cdot Head^2$$

Call **Zero**(GPM : Flow)

Liters = Flow * 3.785

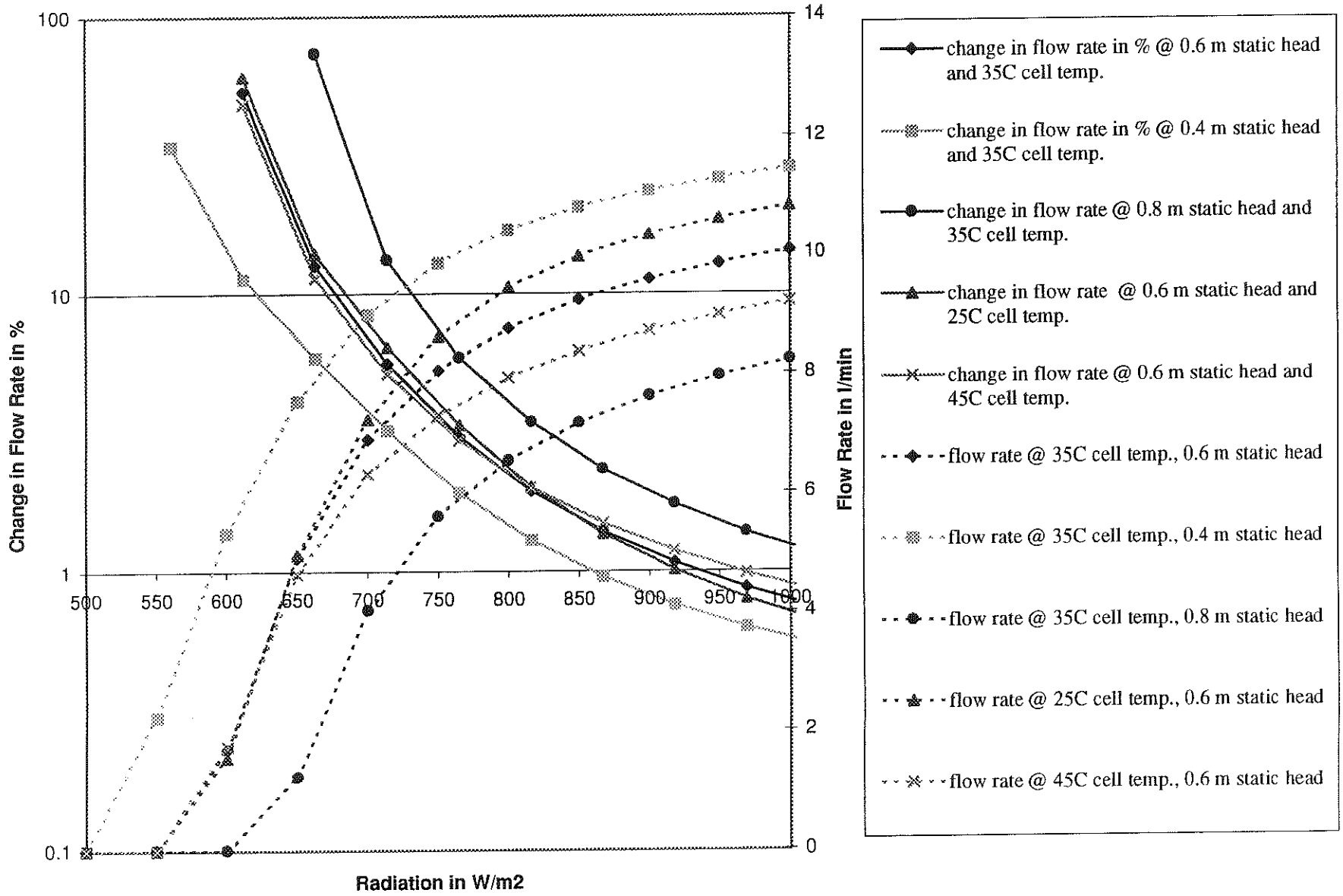

Appendix 5: Effect of a 2% error in radiation on flow rate

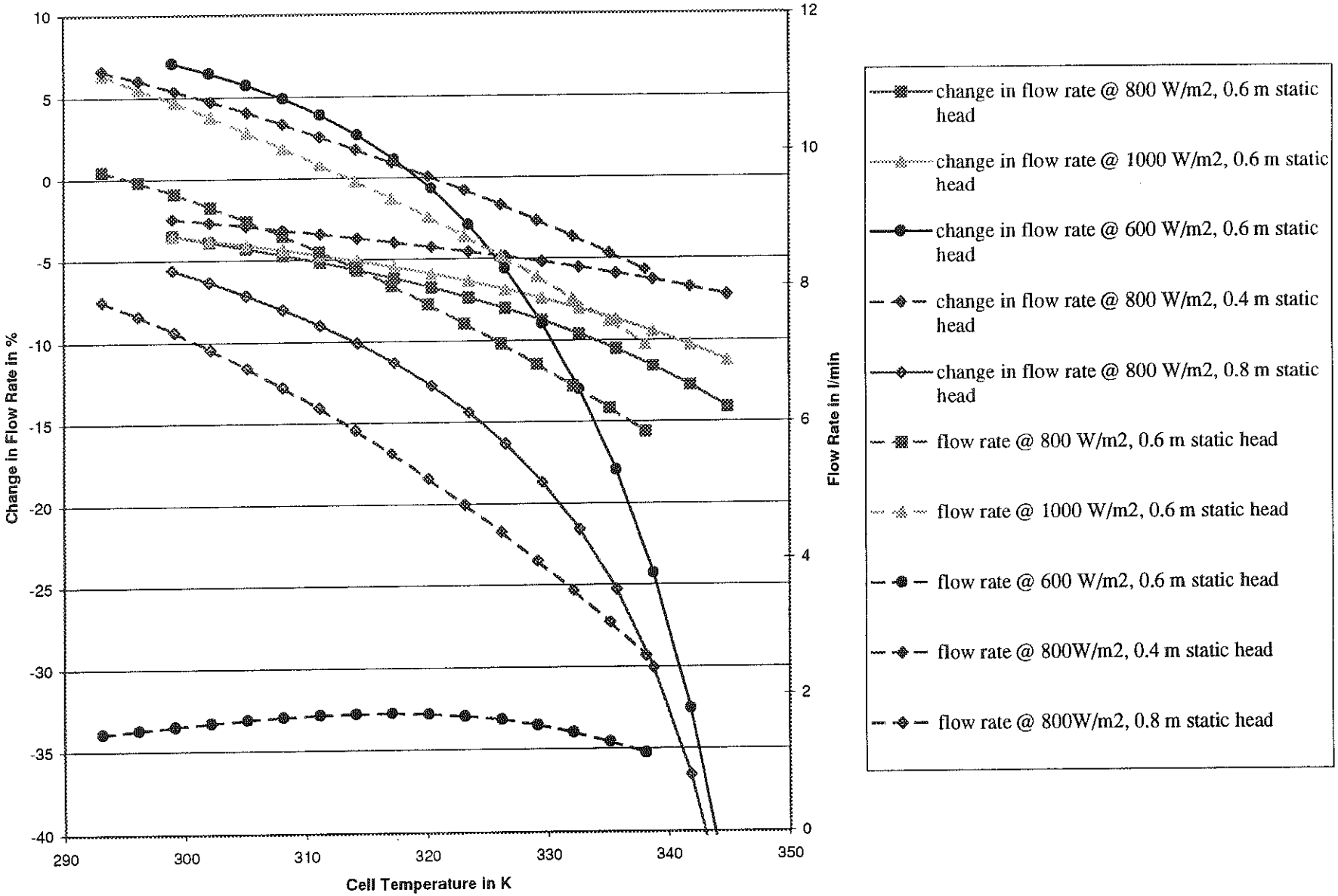

Appendix 6: Effect on a 2% error in cell temperature on flow rate

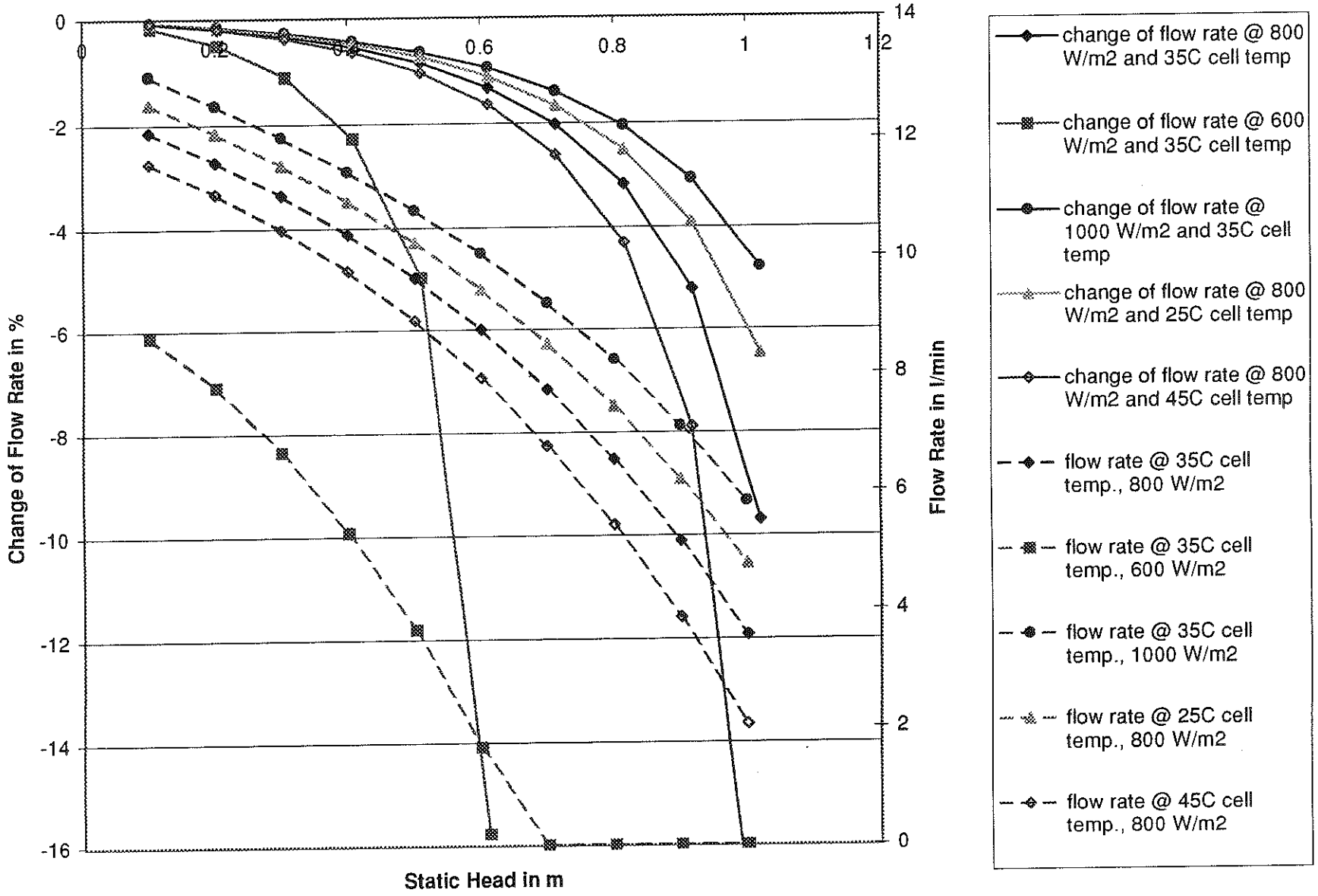

Appendix 7: Effect of a 2% error in static head on flow rate

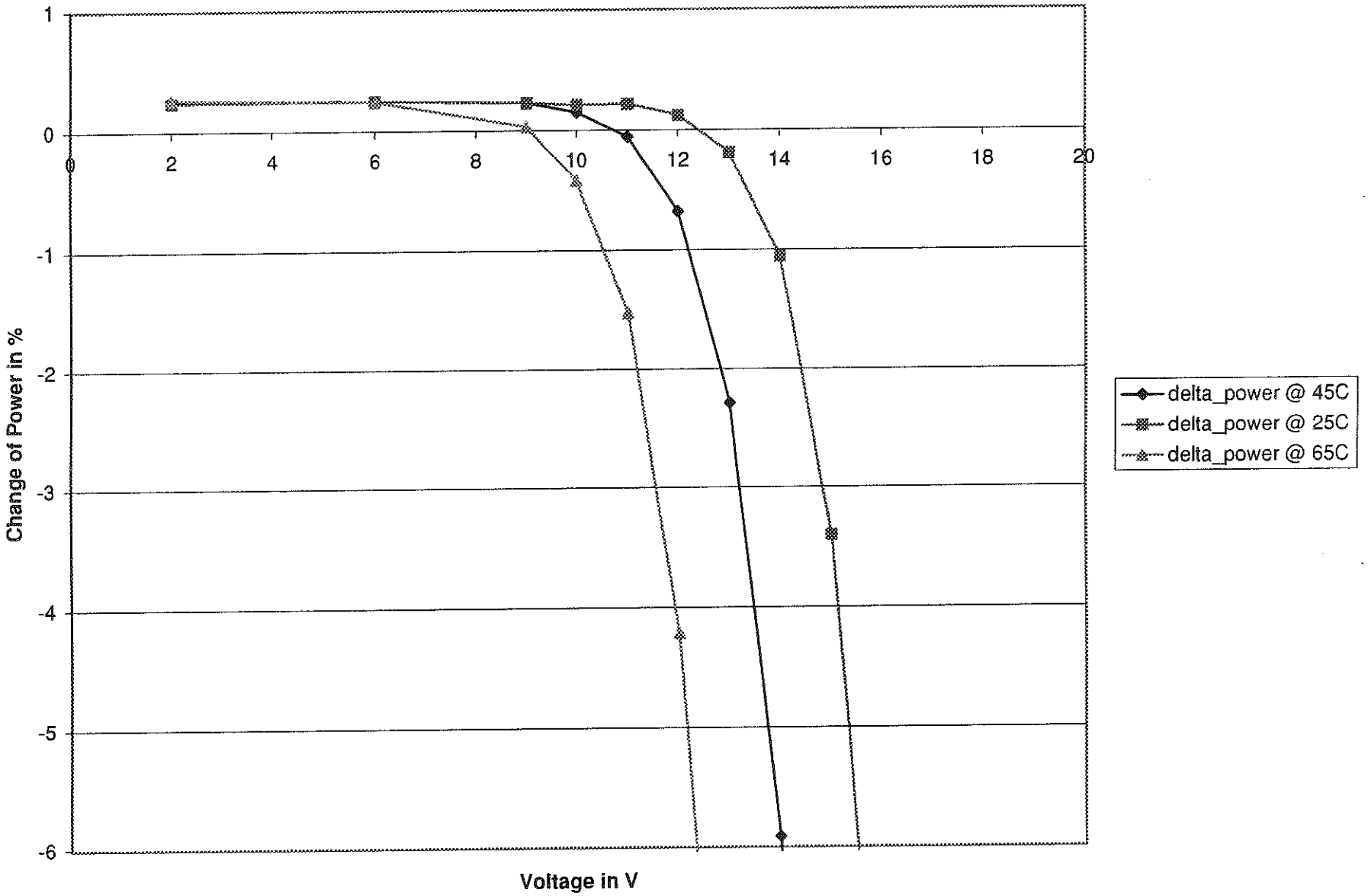

Appendix 8: Effect of a 2% error in cell temperature on power

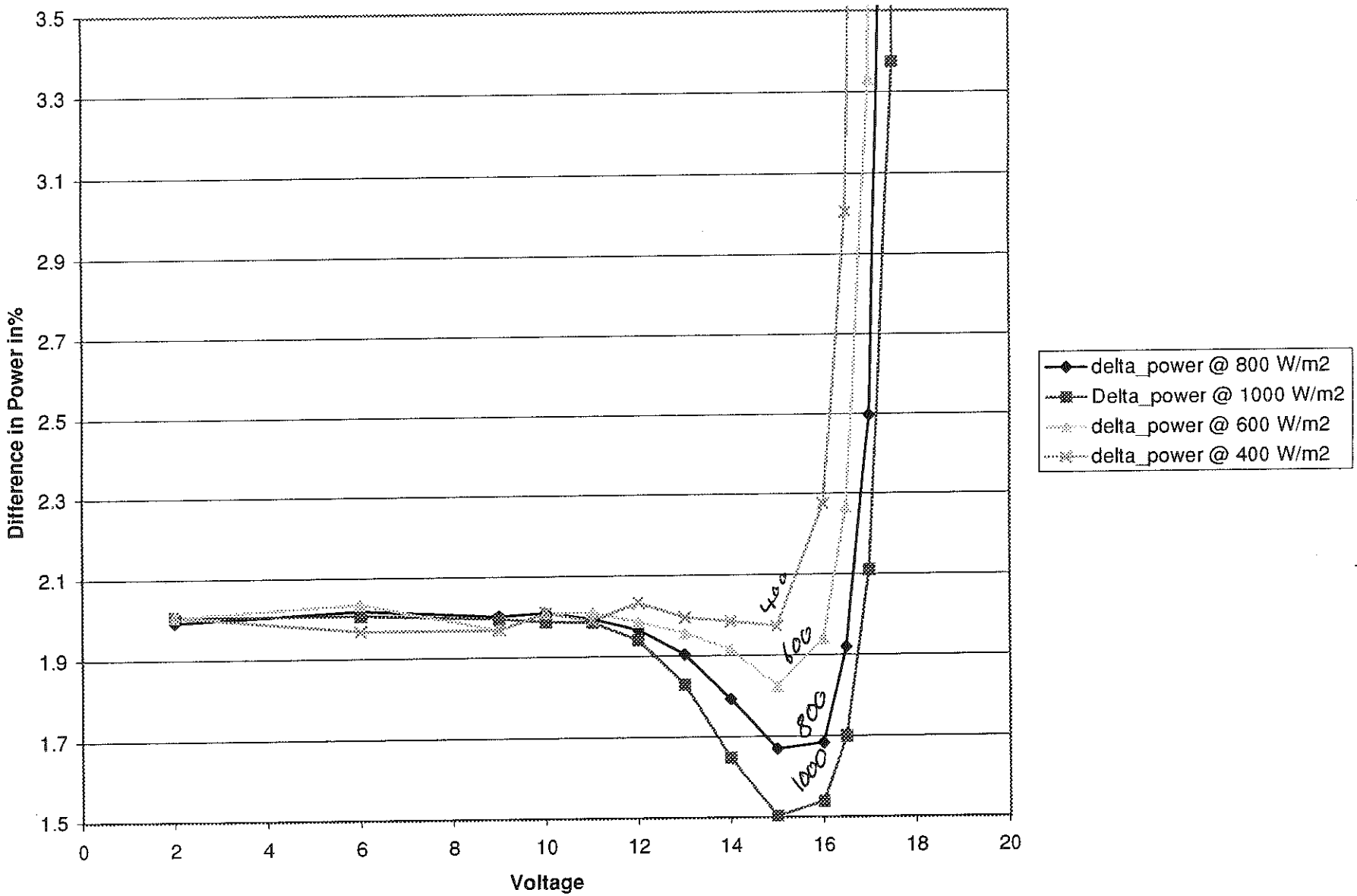

Appendix 9: Effect of a 2% error in radiation on power

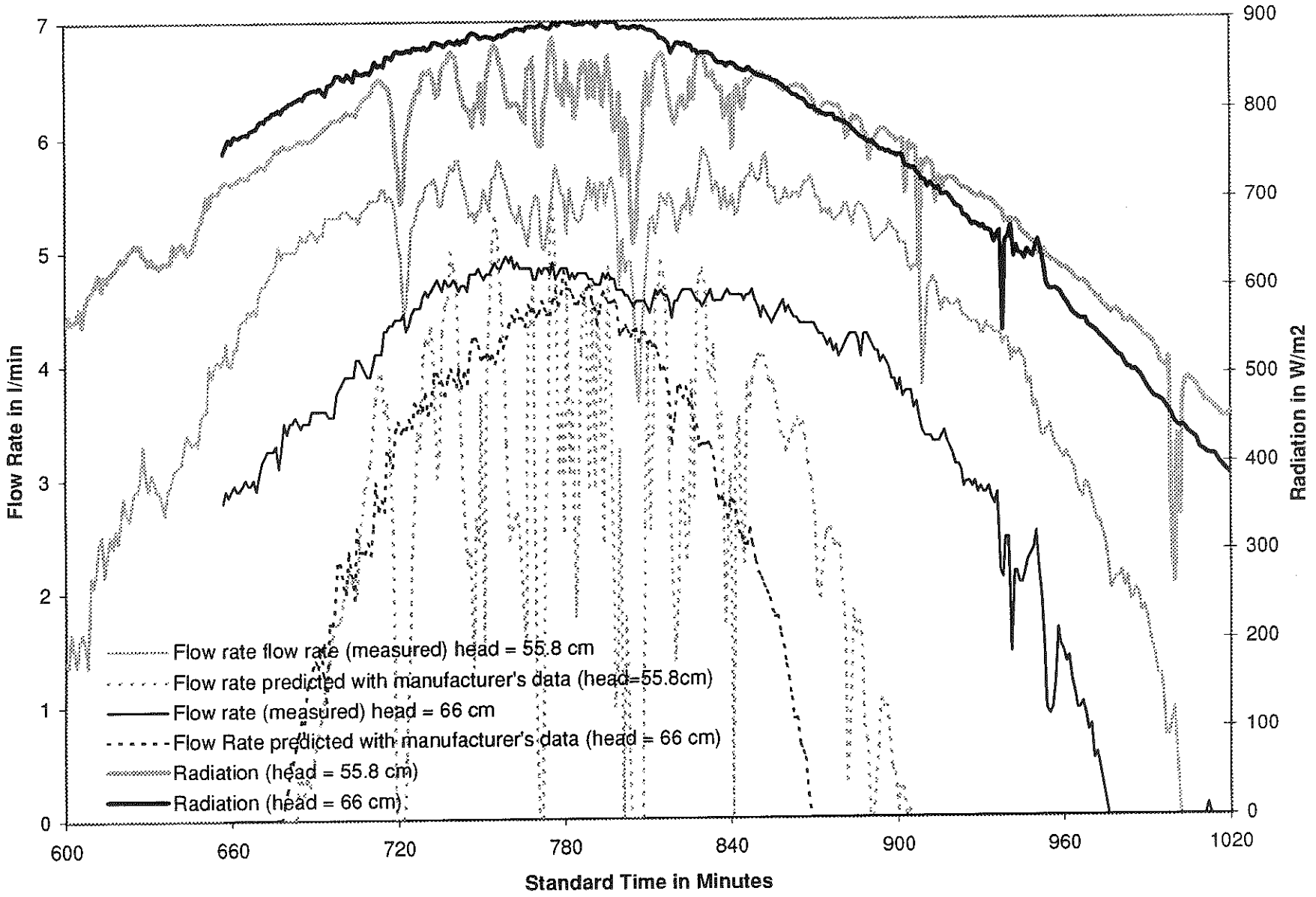

Appendix 10: Radiation and measured and predicted flow rate at two different pump heads over time (SOLAREX)

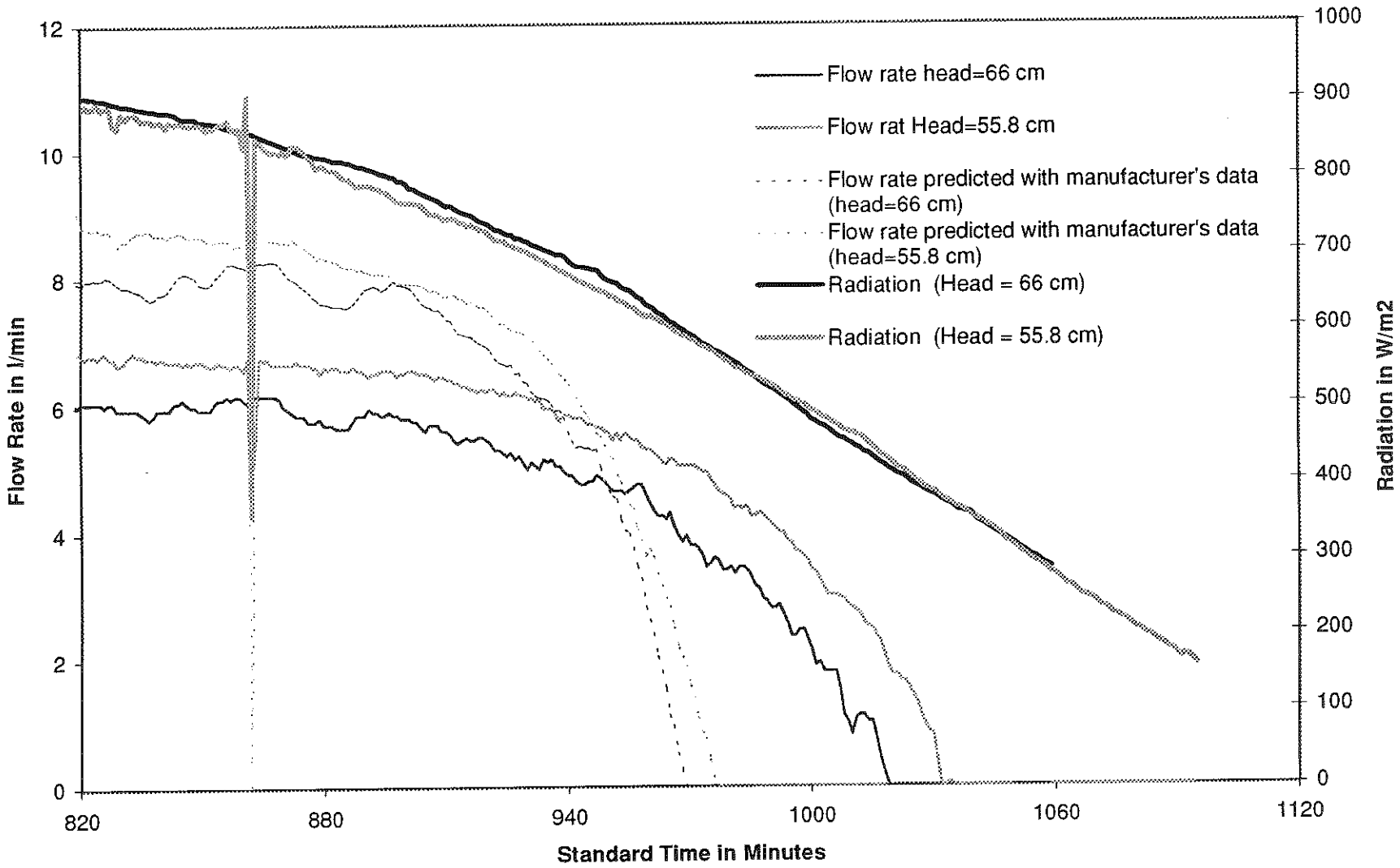

Appendix 11: Radiation and measured and predicted flow rate at two different pump heads over time (SIEMENS)

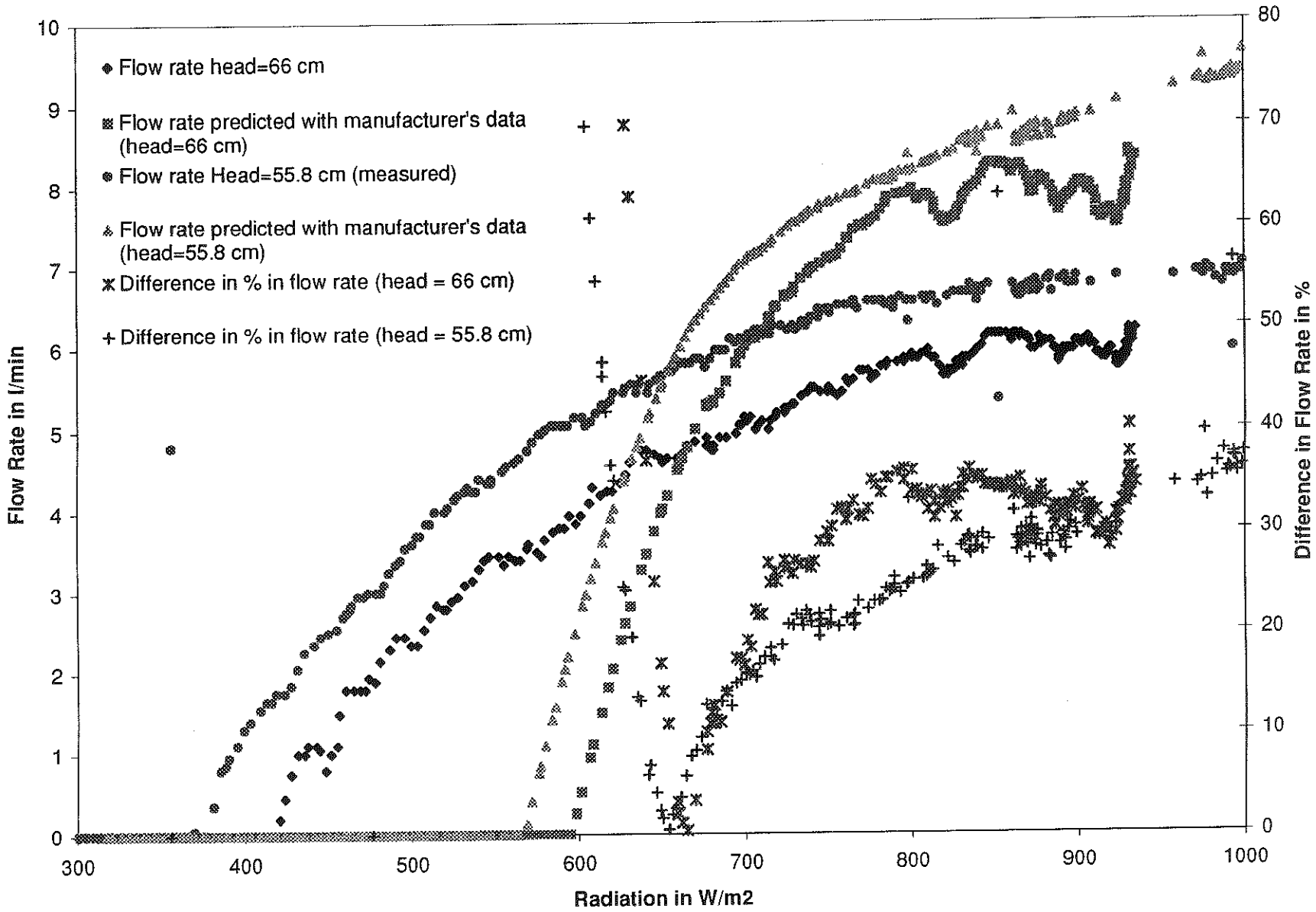

Appendix 12: Flow rate as a function of radiation for two different heads, measurements and predictions with manufacturer's data and difference in % (SIEMENS)

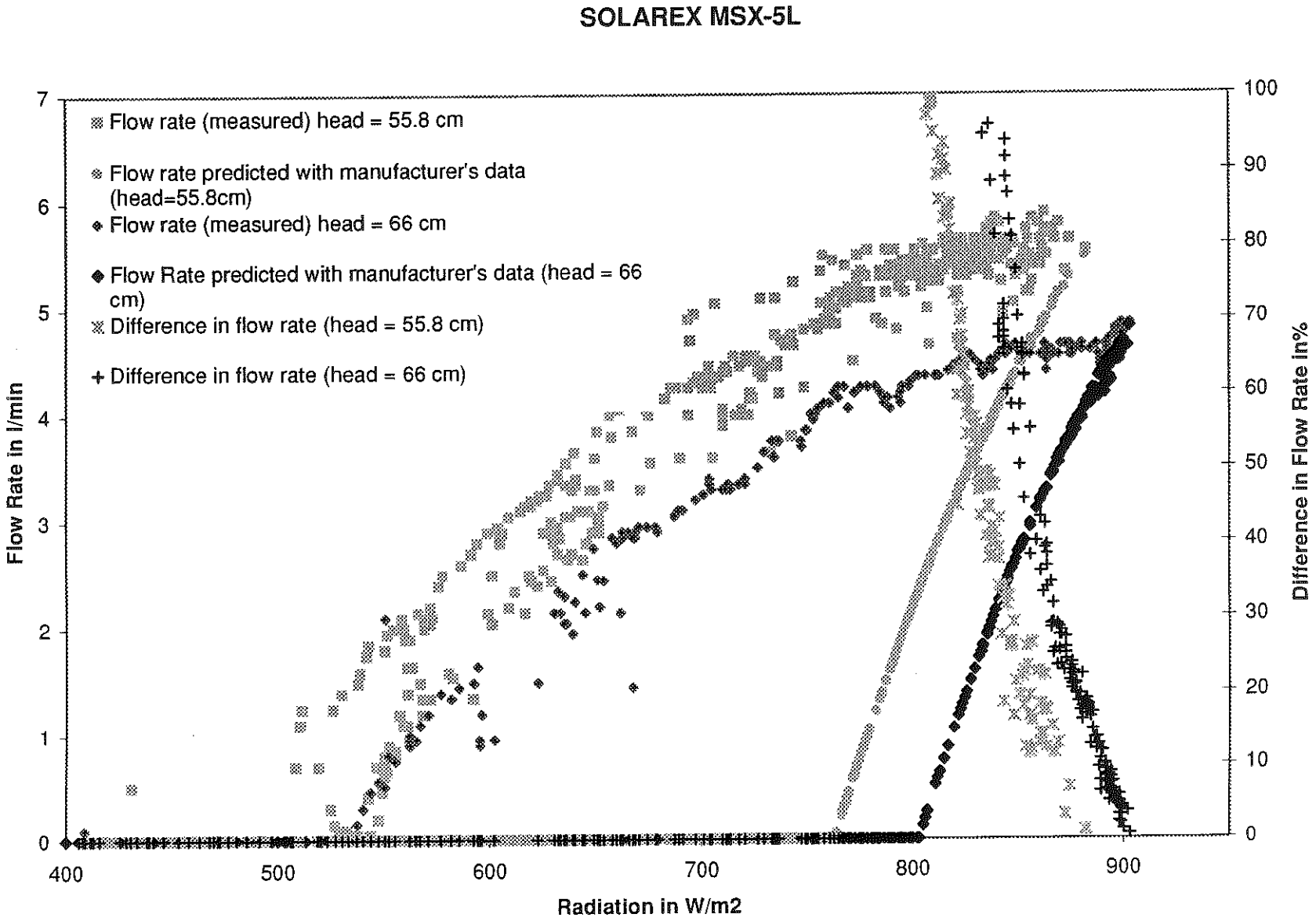

Appendix 13: Flow rate as a function of radiation for two different heads, measurements and predictions with manufacturer's data and difference in % (SOLAREX)

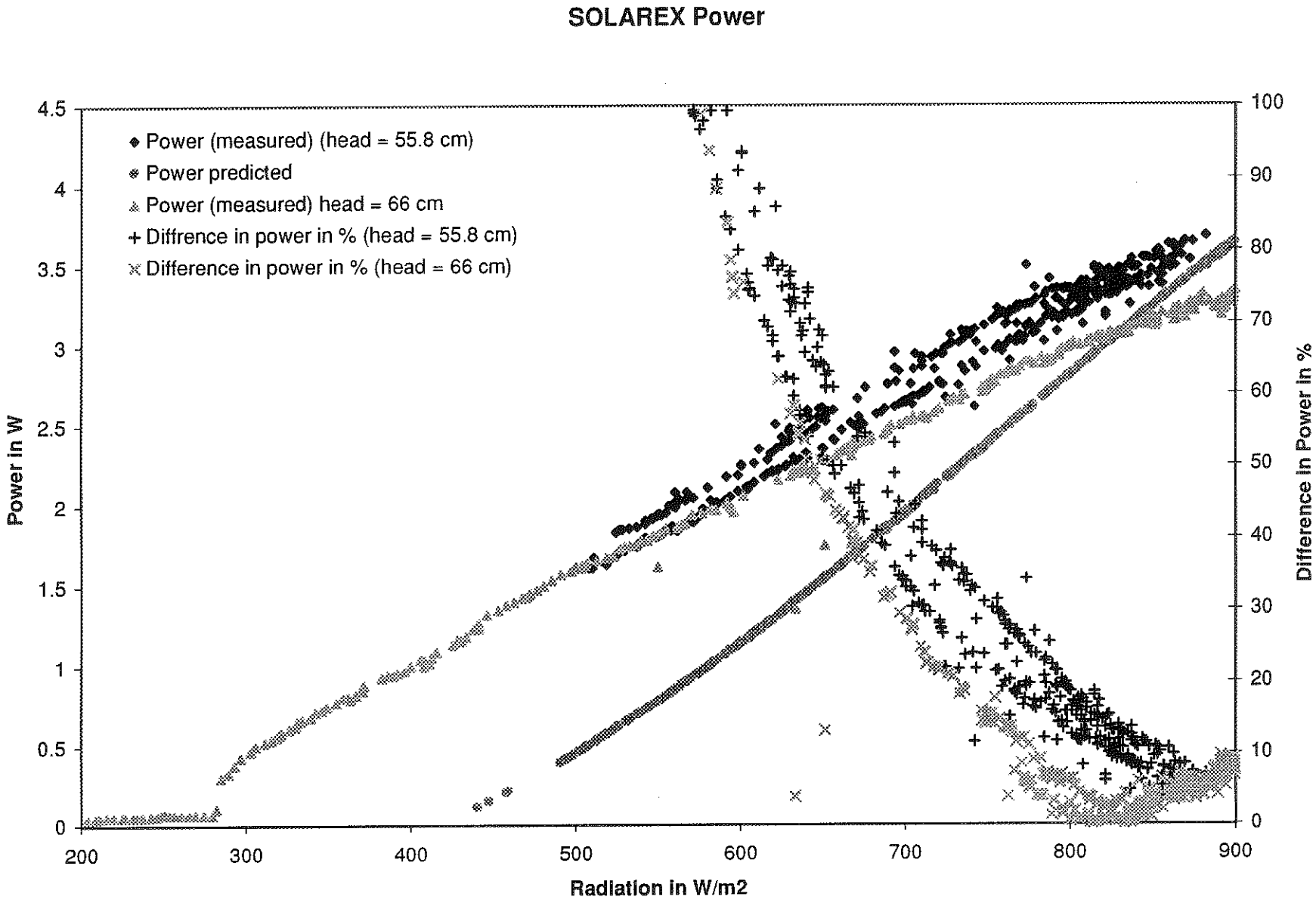

Appendix 14: Measured and predicted power output as a function of radiation at two different pump heads and difference in % (SOLAREX)

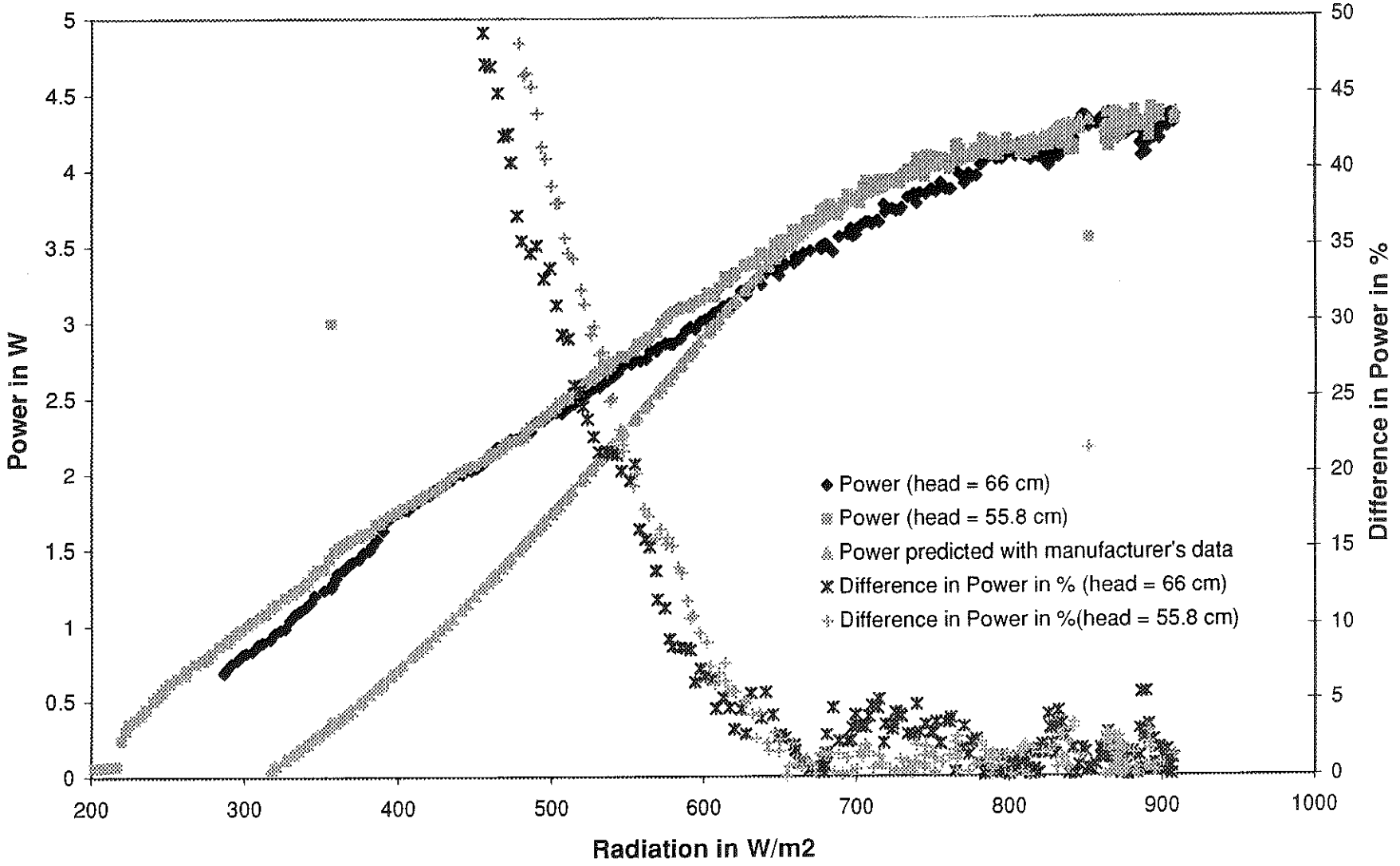

Appendix 15: Measured and predicted power output as a function of radiation at two different pump heads and difference in % (SIEMENS)

$N_s = 33$

$E_q = 1.155$

$Mue_{Isc} = 0.000168$

$R_s = R_{sref}$

$G_{ref} = 1000$

$T_{cref} = 273.2 + 25$

manufacturer's parameters

parameters read from the curve

$n = 1$

$m = 134$

$T_{c,row} = 273.2 + \mathbf{Lookup}(Row, \text{'cell Temp. (SIEMENS)'})$ for $Row = n$ to m

$G_{row} = \mathbf{Lookup}(Row, \text{'modified Radiation'})$ for $Row = n$ to m

$V_{row} = \mathbf{Lookup}(Row, \text{'Voltage'})$ for $Row = n$ to m

$I_{measured,row} = \mathbf{Lookup}(Row, \text{'Current'})$ for $Row = n$ to m

$$xexpv_{row} = \frac{V_{row} + I_{calc,row} \cdot R_s}{A_{row}} - 1 \quad \text{for } Row = n \text{ to } m$$

$$I_{calc,row} = I_{L,row} - I_{0,row} \cdot \mathbf{exp}(xexpv_{row}) \quad \text{for } Row = n \text{ to } m$$

$$I_{L,row} = \frac{G_{row}}{G_{ref}} \cdot (I_{Lref} + Mue_{Isc} \cdot (T_{c,row} - T_{cref})) \quad \text{for } Row = n \text{ to } m$$

$$I_{0,row} = I_{0ref} \cdot \left[\frac{T_{c,row}}{T_{cref}}\right]^3 \cdot \mathbf{exp}\left[N_s \cdot \frac{E_q}{A_{ref}} \cdot \left(1 - \frac{T_{cref}}{T_{c,row}}\right)\right] \quad \text{for } Row = n \text{ to } m$$

$$A_{row} = A_{ref} \cdot \frac{T_{c,row}}{T_{cref}} \quad \text{for } Row = n \text{ to } m$$

$$SSQ = \sum_{j=n}^{m} ((I_{measured,j} - I_{calc,j})^2)$$

$$rms = \sqrt{\frac{SSQ}{m - n + 1}}$$

Appendix 16: EES program for curve fitting measured IV data to the PV model

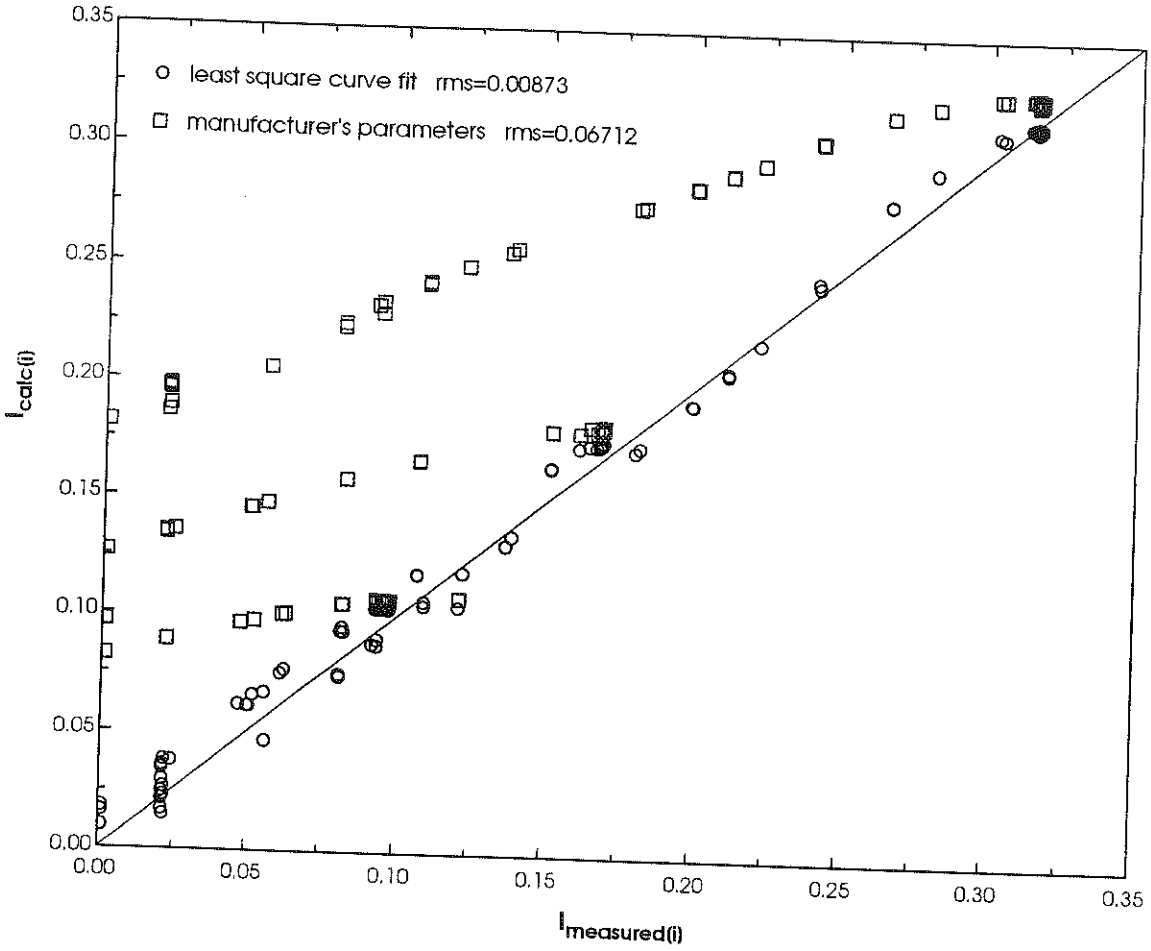

Appendix 17: Calculated vs. measured current with different sets of parameters without incidence angle modifier (SOLAREX)

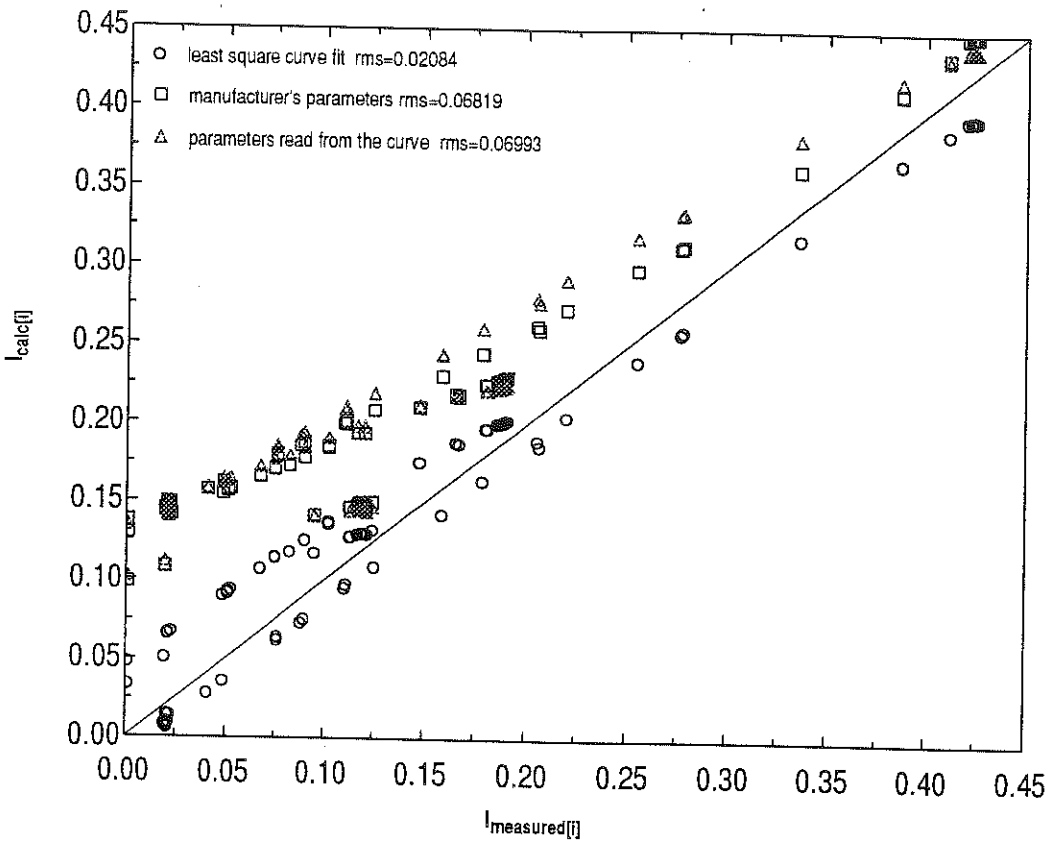

Appendix 18: Calculated vs. measured current with different sets of parameters without incidence angle modifier (SIEMENS)

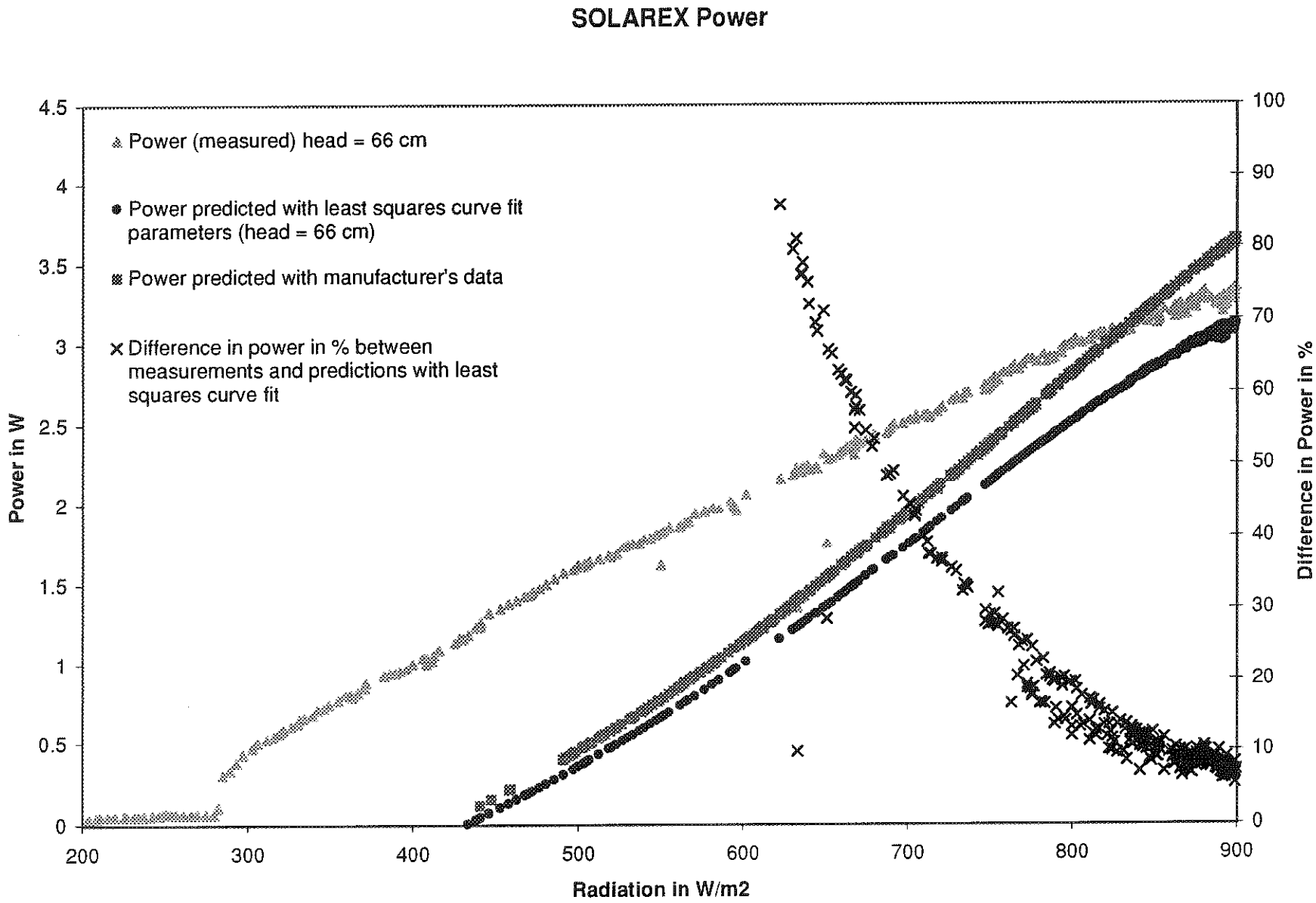

Appendix 19: Measured power and power predicted with manufacturer's data and with least squares curve fit without incidence angle modifier and difference in % (SOLAREX)

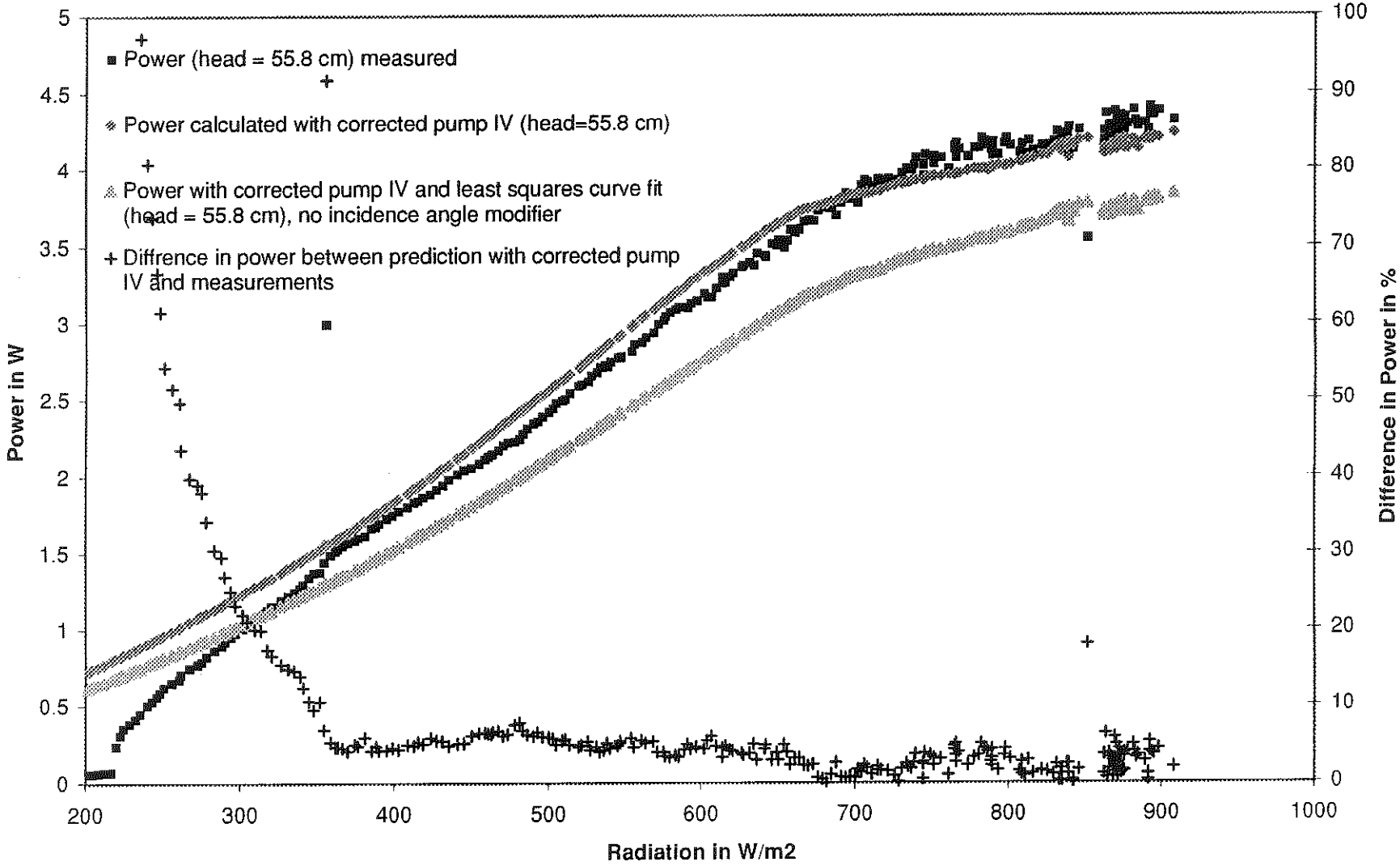

Appendix 20: Measured and predicted power with corrected pump IV characteristics only and with corrected pump IV and least squares curve fit without incidence angle modifier and difference in % at 55.8 cm pump head (SIEMENS)

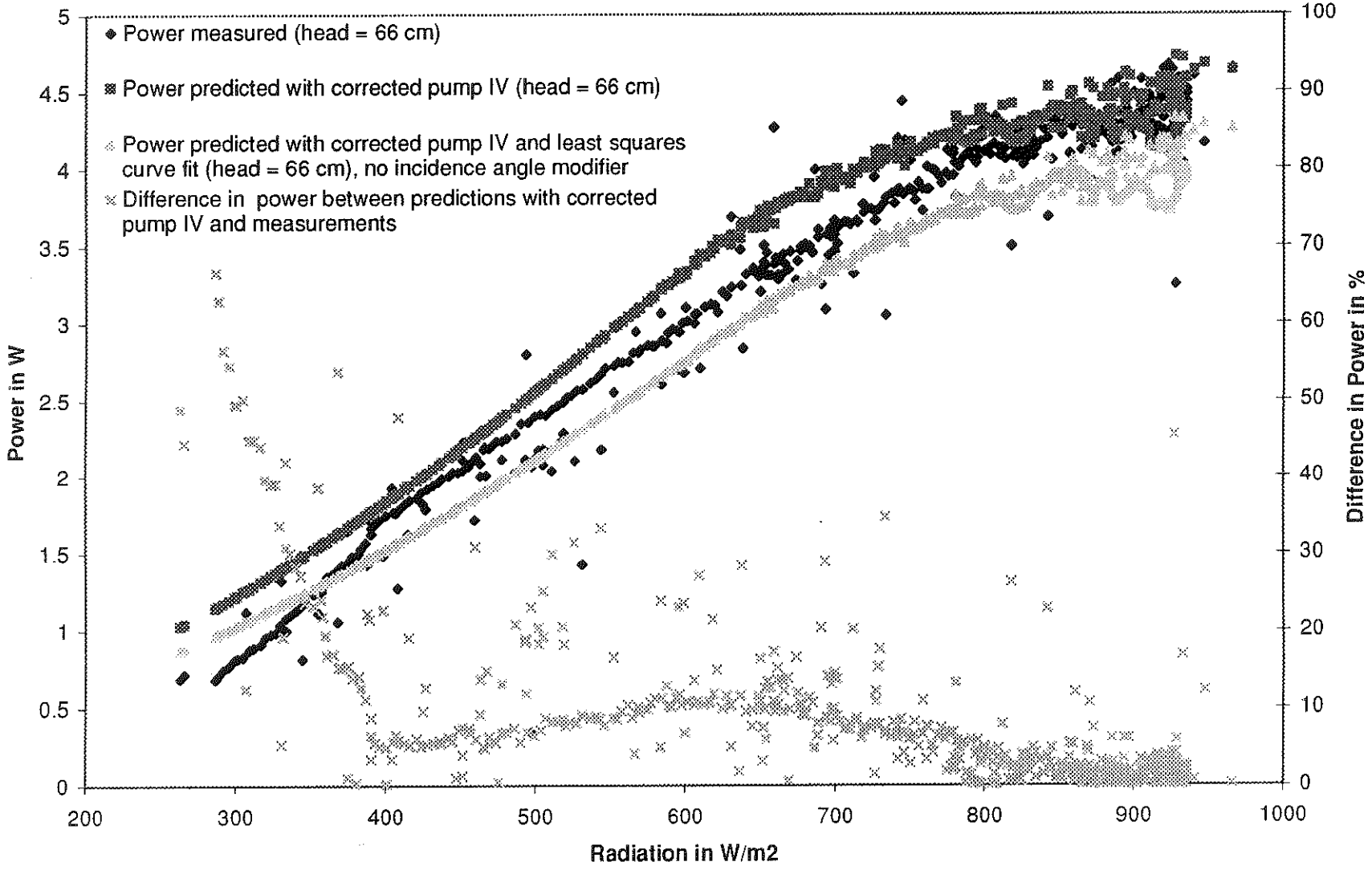

Appendix 21: Measured and predicted power with corrected pump IV characteristics only and with corrected pump IV and least squares curve fit without incidence angle modifier and difference in % at 66 cm pump head (SIEMENS)

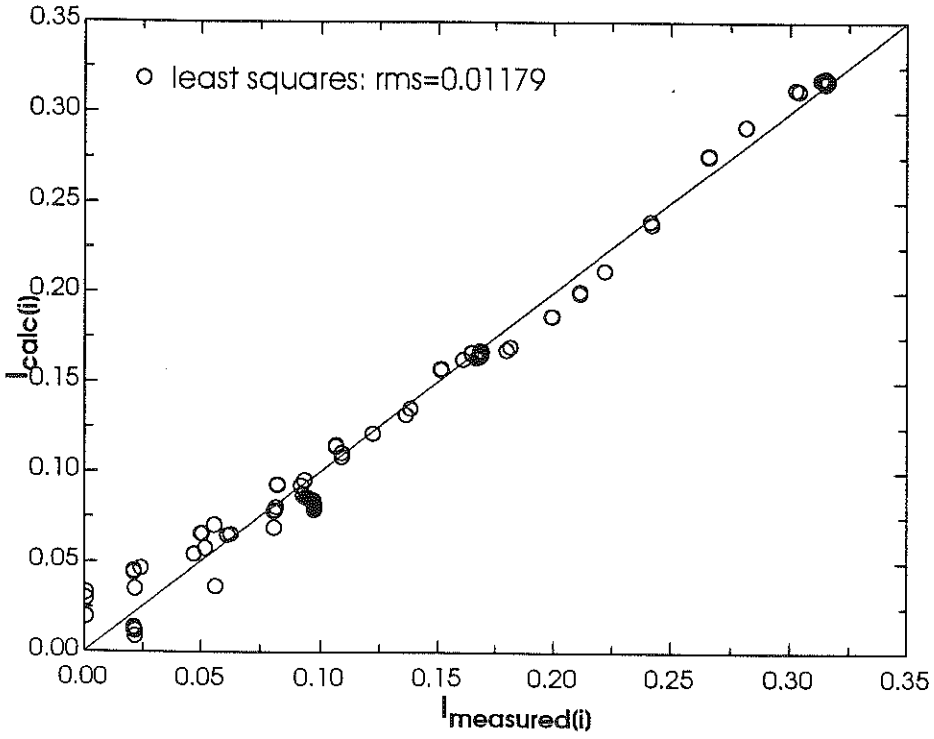

Appendix 22: Calculated over measured current for the least squares curve fit with incidence angle modifier (SOLAREX)

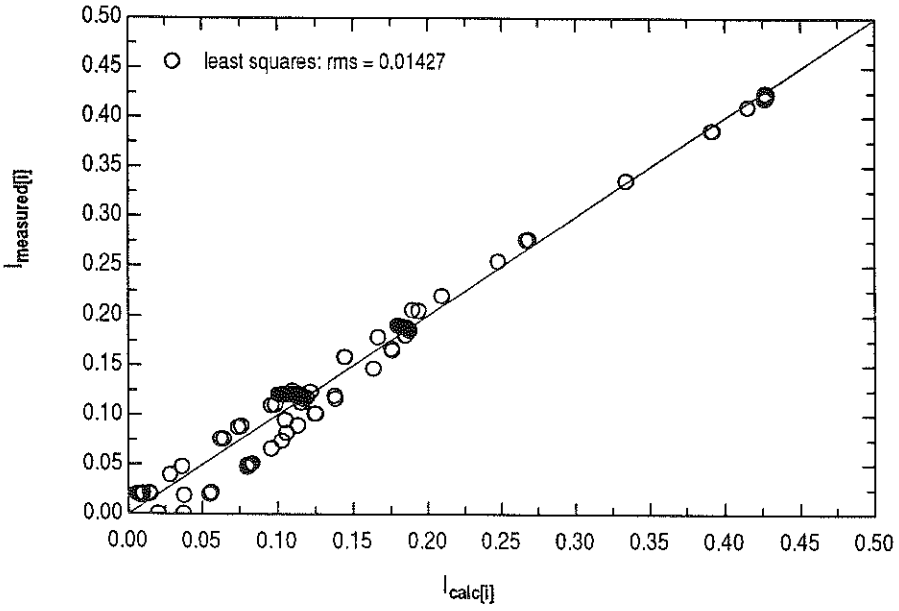

Appendix 23: Calculated over measured current for the least squares curve fit with incidence angle modifier (SIEMENS)

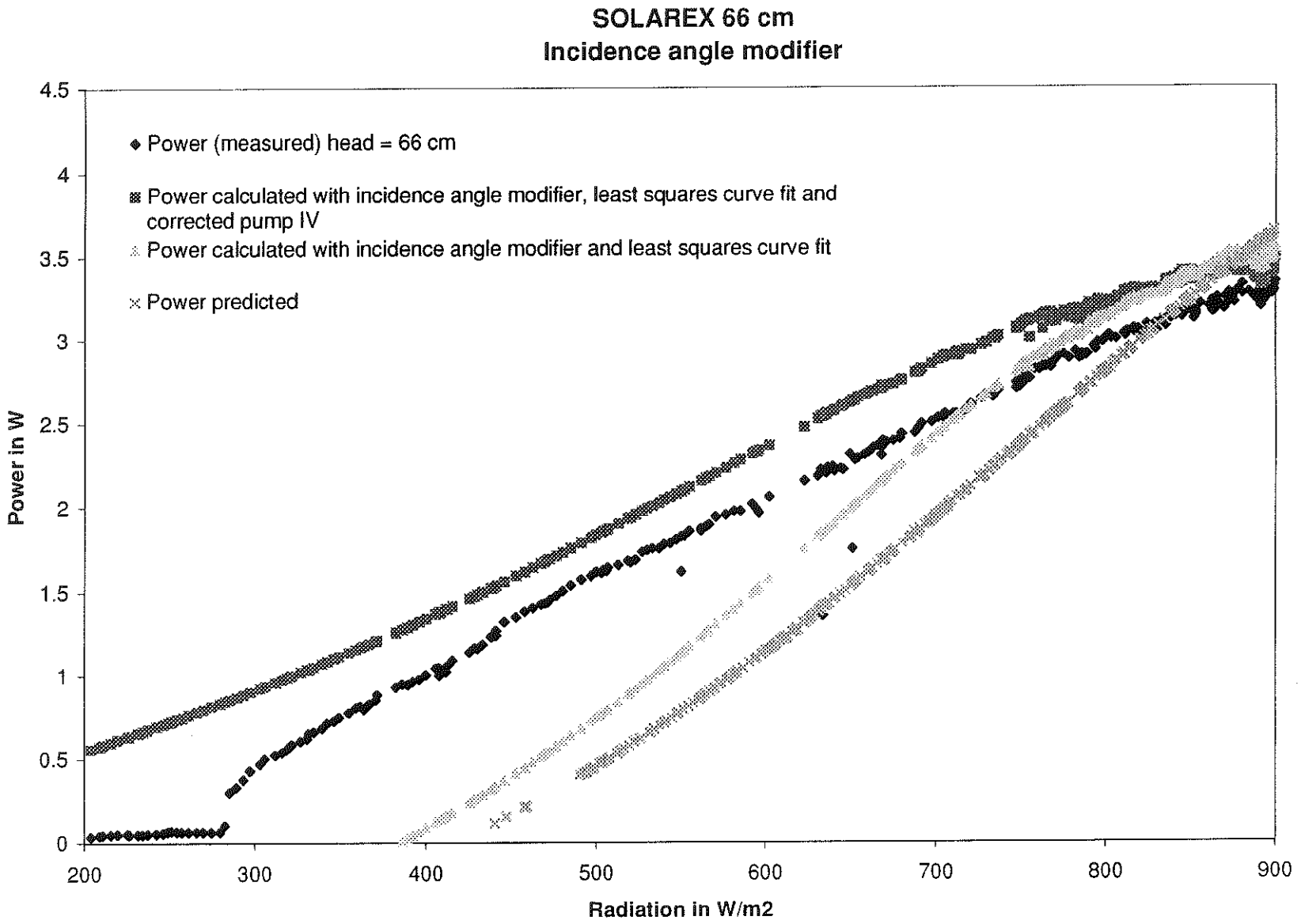

Appendix 24: Measured and predicted power with incidence angle modifier, least squares curve fit and with and without corrected pump IV (SOLAREX)

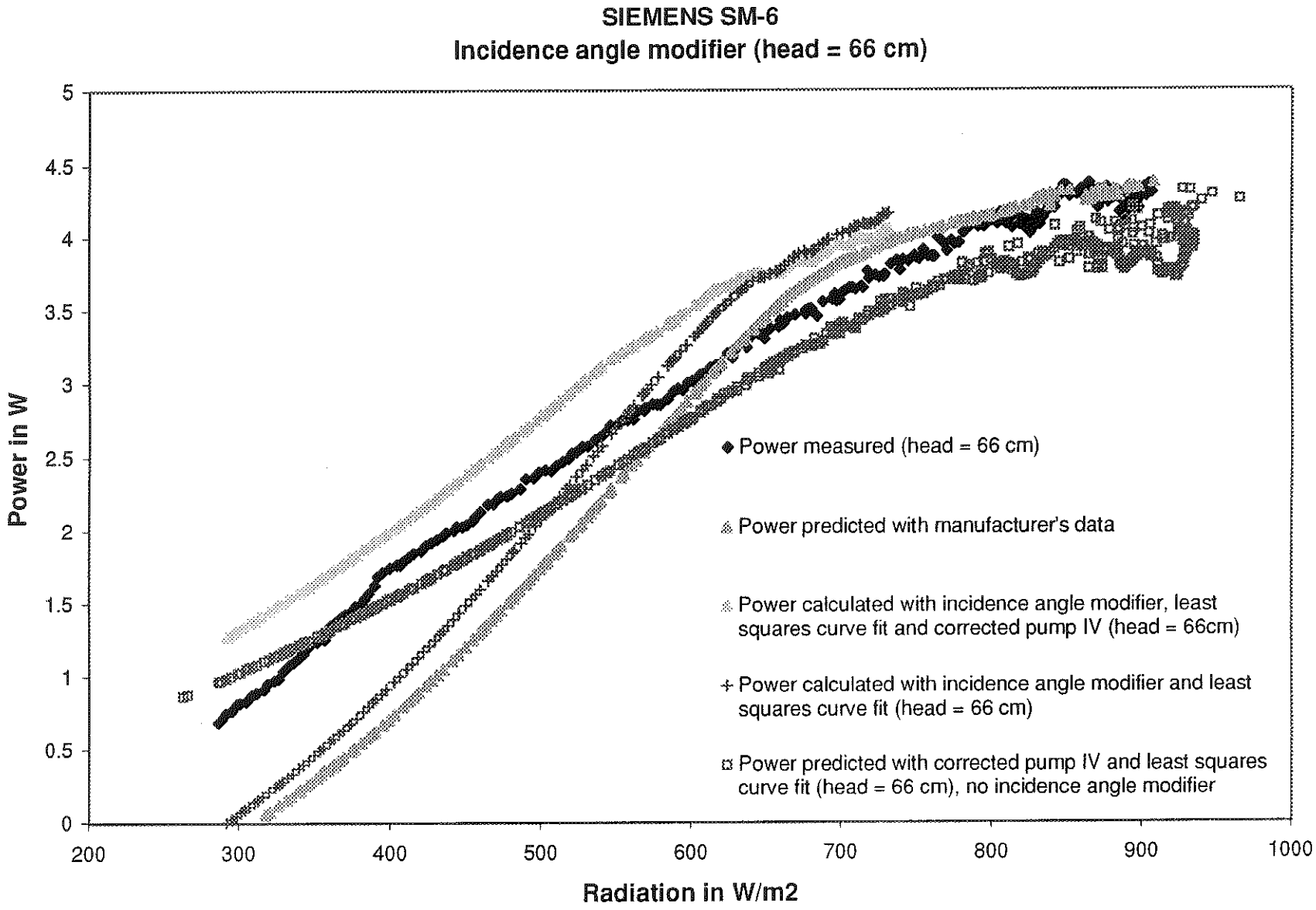

Appendix 25: Measured and predicted power with and without incidence angle modifier, least squares curve fit and corrected pump IV (SIEMENS, head = 66 cm)

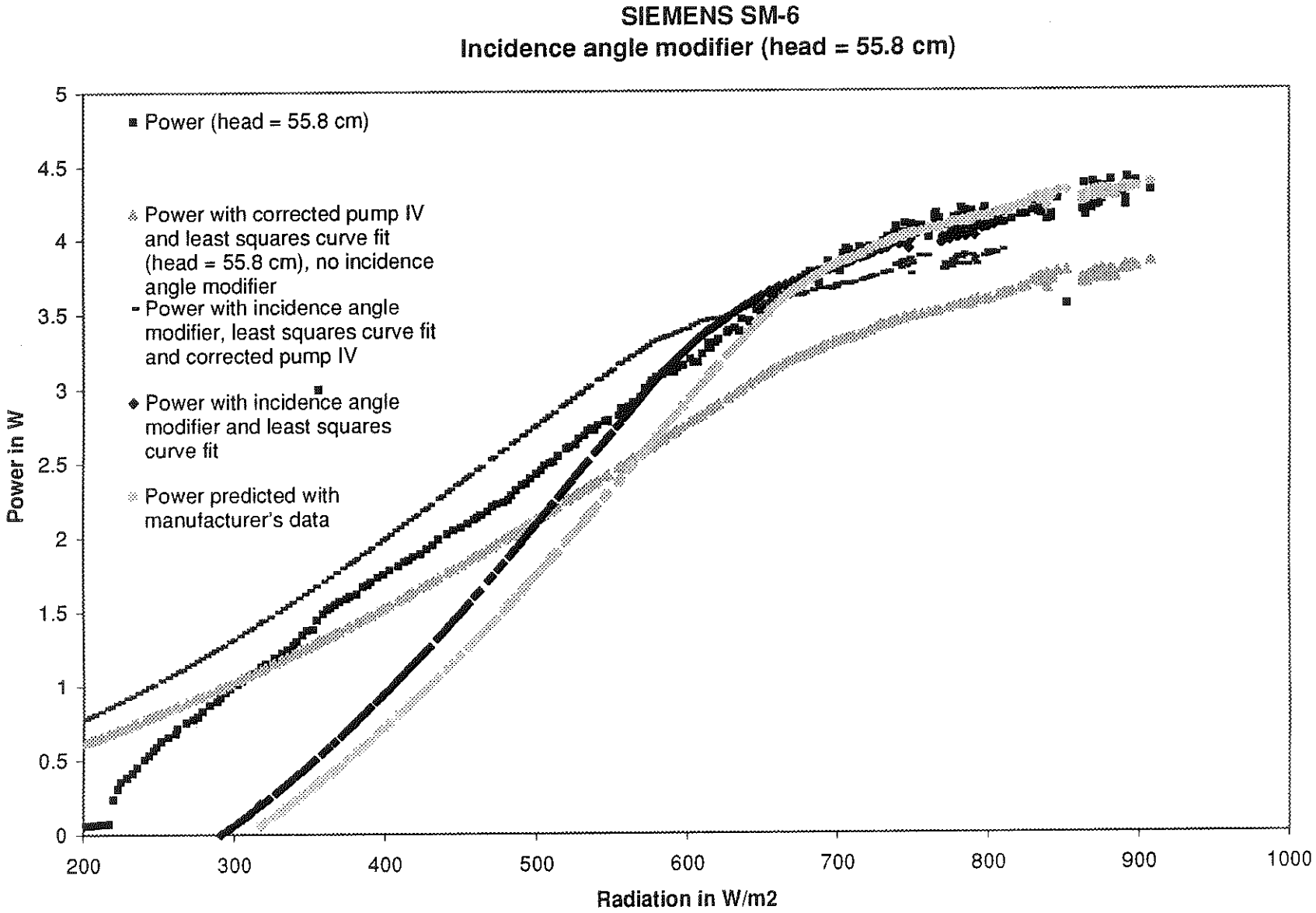

Appendix 26: Measured and predicted power with and without incidence angle modifier, least squares curve fit and corrected pump IV (SIEMENS, head = 55.8cm)

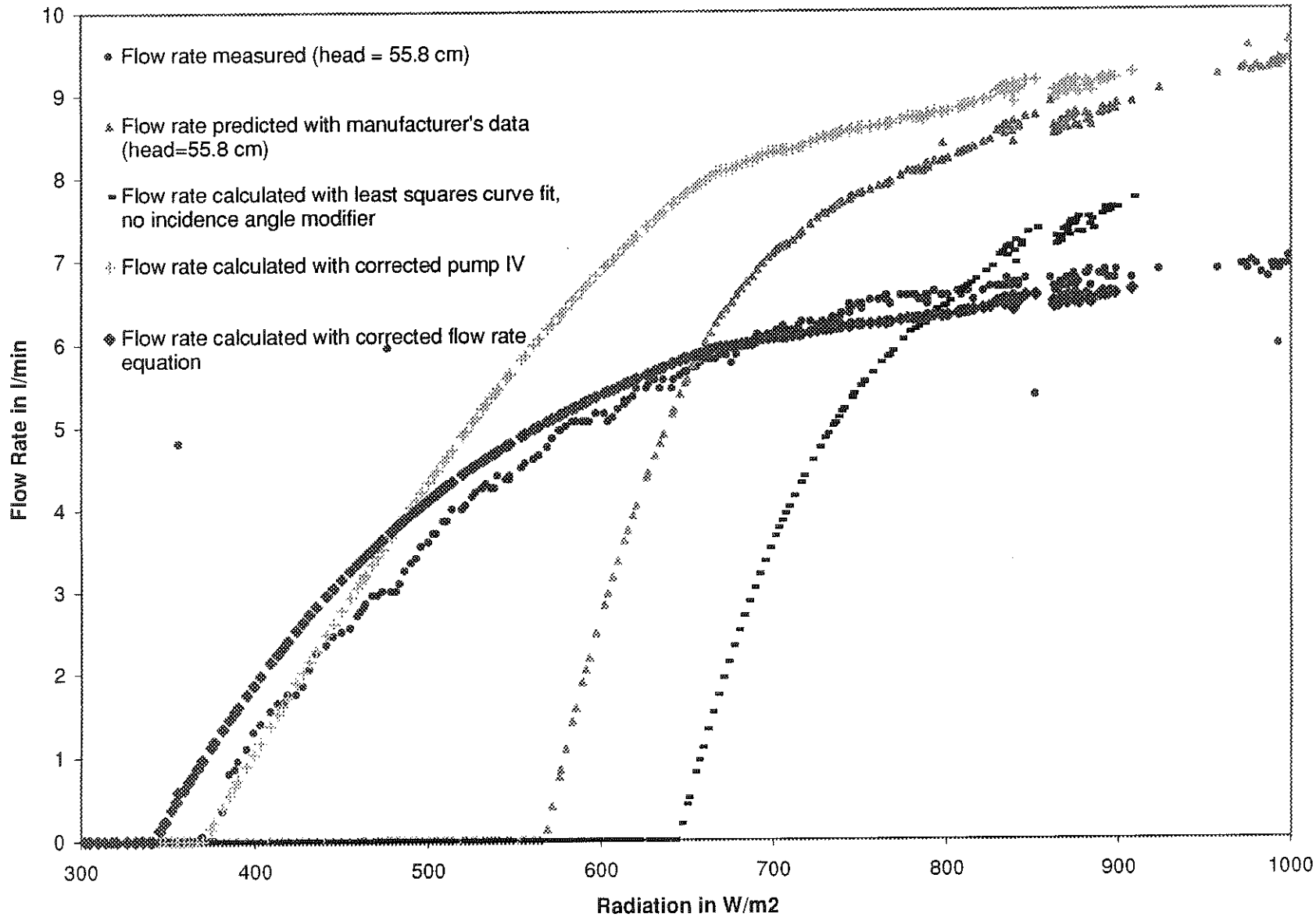

Appendix 27: Measured and predicted flow rate with manufacturer's data, least squares curve fit, corrected pump IV and corrected flow rate equation (SIEMENS)